infection of T cell-tropic HIV-1. Two compounds KRH-2731 and KRH-3955 were found to be highly potent inhibitors for both efficacies without any cytotoxicity or agonistic activity, indicating that they may be promising as anti-cancer metastasis and anti-HIV-1 drugs. In particular, both KRH-2731 and KRH-3955 efficiently inhibited calcium signaling induced by SDF-1α at a concentration of 10 nM, while KRH-3148 and KRH-1636 inhibited at 100 nM and at greater than 10 μM, respectively (Sei Kumakura *et al.*, unpublished results). This indicated that their antagonistic effects were highly correlated with their abilities to inhibit chemotaxis and HIV-1 infection.

While the Jurkat cell line expressed a smaller but almost comparable level of CXCR4 compared with E6-1 cells (Fig. 1a), their migration levels in the presence of SDF-1α were quite different (Fig. 1b). It is possible that the original Jurkat cells express non-functional CXCR4 with regard to signal transduction that is required for chemotaxis.

Tumor cells from various types of human cancers of epithelial, mesenchymal, and hematopoietic origins express high levels of CXCR4.[14,16] The interaction of SDF-1α with its receptor CXCR4 contributes to metastasis of breast cancer as well as a number of other malignancies in the lung, brain, and prostate. Furthermore, patients with cancers expressing high levels of CXCR4 have more extensive metastasis at lymph nodes compared with low CXCR4-expressing ones.[22] On this basis, the efficient CXCR4 antagonists demonstrated in this study may be highly valuable for the regulation of cancer metastasis. In fact, a synthetic peptide against CXCR4 efficiently inhibited metastasis of breast cancer in a mouse model,[21] thus providing support to our notion. However, a hurdle remains for the delivery of the peptide inihibitor to the primary focus of cancer in patients, thus impeding the clinical application of the inhibitor. In this regard, our low molecular weight CXCR4 antagonists are promising because they are non-cytotoxic and can be administered orally. In fact, KRH-3955 showed oral bioavailability of 25.6% in rats and its oral administration blocked X4 HIV-1 replication in the human peripheral blood lymphocytes and in severe combined immunodeficiency mouse system (Tsutomu Murakami *et al.*, manuscript in preparation). It is notable that AMD3100, another small non-peptide CXCR4 antagonist, has been shown to inhibit metastasis of cancer cells *in vitro* and *in vivo*.[23,24] Moreover, our preliminary data suggested that injection of the breast cancer cell line MDA-231 produced a huge tumor at the inoculated site as well as aggressive metastasis in the lungs of mice, and that our compounds partially inhibited both the primary tumor growth and the metastasis (data not shown).

In conclusion, CXCR4 antagonists, which can be orally administered, are promising agents for SDF-1α-mediated metastasis of cancer cells and also for the treatment and prophylaxis of a number of diseases related to the interaction between CXCR4 and SDF-1α, the best example of which would be an anti-HIV-1 drug.

Acknowledgments

We thank M. Kannagi and S. Yamaoka, Tokyo Medical and Dental University, for critical discussions. This work was supported by grants from the Ministry of Education, Culture, Sports, Science and Technology; the Ministry of Health, Labor and Welfare; and Human Health Science of Japan.

References

1 Ward SG, Westwick J. Chemokines: understanding their role in T-lymphocyte biology. *Biochem J* 1998; **333**: 457–70.
2 Le Y, Zhou Y, Iribarren P *et al.* Chemokines and chemokine receptors: their manifold roles in homeostasis and disease. *Cell Mol Immunol* 2004; **1**: 95–104.
3 Burger JA, Kipps TJ. CXCR4: a key receptor in the cross-talk between tumor cells and their microenvironment. *Blood* 2006; **107**: 1761–7.
4 Horuk R. Chemokine receptors. *Cytokine Growth Factor Rev* 2001; **12**: 313–15.
5 Nagasawa T, Hirota S, Tachibana K *et al.* Defects of B-cell lymphopoiesis and bone-marrow myelopoiesis in mice lacking the CXC chemokine PBSF/SDF-1. *Nature* 1996; **382**: 635–8.
6 Tachibana K, Hirota S, Iizasa H *et al.* The chemokine receptor CXCR4 is essential for vascularization of the gastrointestinal tract. *Nature* 1998; **393**: 591–4.
7 Zou YR, Kottmann AH, Kuroda M *et al.* Function of the chemokine receptor CXCR4 in haematopoiesis and in cerebellar development. *Nature* 1998; **393**: 595–9.
8 Burns JM, Summers BC, Wang Y *et al.* A novel chemokine receptor for SDF-1 and I-TAC involved in cell survival, cell adhesion, and tumor development. *J Exp Med* 2006; **203**: 2201–13.
9 Berger EA, Murphy PM, Farber JM. Chemokine receptors as HIV-1 coreceptors: roles in viral entry, tropism, and disease. *Annu Rev Immunol* 1999; **17**: 657–700.
10 Su L, Kaneshima H, Bonyhadi M *et al.* HIV-1-induced thymocyte depletion is associated with indirect cytopathogenicity and infection of progenitor cells in vivo. *Immunity* 1995; **2**: 25–36.
11 Bleul CC, Farzan M, Choe H *et al.* The lymphocyte chemoattractant SDF-1 is a ligand for LESTR/fusin and blocks HIV-1 entry. *Nature* 1996; **382**: 829–33.
12 Alkhatib G, Combadiere C, Broder CC *et al.* CC CKR5: a RANTES, MIP-1 alpha, MIP-1bata receptor as a fusion cofactor for macrophage-tropic HIV-1. *Science* 1996; **272**: 1955–8.
13 Cocchi F, DeVico AL, Garzino-Demo A *et al.* Identification of RANTES, MIP-1 alpha, and MIP-1 beta as the major HIV-suppressive factors produced by $CD8^+$ T cells. *Science* 1995; **270**: 1811–15.
14 Balkwill F. Cancer and the chemokine network. *Nature Rev Cancer* 2004; **4**: 540–50.
15 Luker KE, Luker GD. Functions of CXCL12 and CXCR4 in breast cancer. *Cancer Lett* 2006; **238**: 30–41.
16 Muller A, Homey B, Soto H *et al.* Involvement of chemokine receptors in breast cancer metastasis. *Nature* 2001; **410**: 50–6.
17 Liotta LA. An attractive force in metastasis. *Nature* 2001; **410**: 24–5.
18 Santiago B, Baleux F, Palao G *et al.* CXCL12 is displayed by rheumatoid endothelial cells through its base amino-terminal motif on heparan sulfate proteoglycans. *Arthritis Res Ther* 2006; **8**: R43.
19 Ichiyama K, Yokoyama-Kumakura S, Tanaka Y *et al.* A duodenally absorbable CXC chemokine receptor 4 antagonist, KRH-1636, exhibits a potent and selective anti-HIV-1 activity. *Proc Natl Acad Sci USA* 2003; **100**: 4185–90.
20 Tamamura H, Hori A, Kanzaki N *et al.* T140 analogs as CXCR4 antagonists identified as anti-metastatic agents in the treatment of breast cancer. *FEBS Lett* 2003; **550**: 79–83.
21 Liang Z, Wu T, Lou H *et al.* Inhibition of breast cancer metastasis by selective synthetic polypeptide against CXCR4. *Cancer Res* 2004; **64**: 4302–8.
22 Dewan MZ, Ahmed S, Iwasaki Y *et al.* Stromal cell-derived factor-1 and CXCR4 receptor interaction in tumor growth and metastasis of breast cancer. *Biomed Pharmacother* 2006; **60**: 273–6.
23 Yoon Y, Liang Z, Zhang X *et al.* CXC chemokine receptor-4 antagonist blocks both growth of primary tumor and metastasis of head and neck cancer in xenograft mouse models. *Cancer Res* 2007; **67**: 7518–24.
24 Li JK, Yu L, Shen Y *et al.* Inhibition of CXCR4 activity with AMD3100 decreases invasion of human colorectal cancer cells *in vitro*. *World J Gastroenterol* 2008; **14**: 2308–13.

Journal of Cellular Physiology

Dys-Regulated Activation of a Src Tyroine Kinase Hck at the Golgi Disturbs *N*-Glycosylation of a Cytokine Receptor Fms

RANYA HASSAN,[1] SHINYA SUZU,[1] MASATERU HIYOSHI,[1] NAOKO TAKAHASHI-MAKISE,[1] TAKAMASA UENO,[2] TSUTOMU AGATSUMA,[3] HIROFUMI AKARI,[4] JUN KOMANO,[5] YUTAKA TAKEBE,[6] KAZUO MOTOYOSHI,[7] AND SEIJI OKADA[1]*

[1]*Division of Hematopoiesis, Center for AIDS Research, Kumamoto University, Kumamoto, Kumamoto, Japan*

[2]*Viral Immunology, Center for AIDS Research, Kumamoto University, Kumamoto, Kumamoto, Japan*

[3]*Tokyo Research Laboratories, Kyowa Hakko Co., Ltd, Machida, Tokyo, Japan*

[4]*Laboratory of Disease Control, Tsukuba Primate Research Center, National Institute of Biomedical Innovation, Tsukuba, Ibaraki, Japan*

[5]*Laboratory of Virology and Pathogenesis, AIDS Research Center, National Institute of Infectious Diseases, Shinjuku, Tokyo, Japan*

[6]*Laboratory of Molecular Biology and Epidemiology, AIDS Research Center, National Institute of Infectious Diseases, Shinjuku, Tokyo, Japan*

[7]*Department of Internal Medicine, National Defense Medical College, Tokorozawa, Saitama, Japan*

HIV-1 Nef accelerates the progression to AIDS by binding with and activating a Src kinase Hck, but underlying molecular basis is not understood. We revealed that Nef disturbed *N*-glycosylation/trafficking of a cytokine receptor Fms in an Hck-dependent manner, a possible trigger to worsen uncontrolled immune system. Here, we provide direct evidence that dys-regulated activation of Hck pre-localized to the Golgi apparatus causes this Fms maturation arrest. A striking change in Hck induced by Nef other than activation was its skewed localization to the Golgi due to predominant Golgi-localization of Nef. Studies with different Nef alleles and their mutants showed a clear correlation among higher Nef-Hck affinity, stronger Hck activation, severe Golgi-localization of Hck and severe Fms maturation arrest. Studies with a newly discovered Nef-Hck binding blocker 2c more clearly showed that skewed Golgi-localization of active Hck was indeed the cause of Fms maturation arrest. 2c blocked Nef-induced skewed Golgi-localization of an active form of Hck (Hck-P2A) and Fms maturation arrest by Nef/Hck-P2A, but showed no inhibition on Hck-P2A kinase activity. Our finding establishes an intriguing link between the pathogenesis of Nef and a newly emerging concept that the Golgi-localized Src kinases regulate the Golgi function.

J. Cell. Physiol. 221: 458–468, 2009.

Studies of HIV-1-infected patients and monkey models have demonstrated that Nef, a protein with no enzymatic activity encoded by the HIV-1 genome, is a critical determinant for the development of AIDS (Kestler et al., 1991; Deacon et al., 1995; Kirchhoff et al., 1995). Subsequent studies of HIV-1 transgenic (Tg) mice supported the idea. The expression of entire coding sequences of HIV-1 in $CD4^+$ T cells and macrophages caused an AIDS-like disease, which was abolished by Nef deletion (Hanna et al., 1998). This pathogenetic activity of Nef is supposed to be mediated by its binding with cellular proteins, and a well-defined partner of Nef is Hck (Saksela et al., 1995), a member of Src family tyrosine kinases expressed in macrophages. Other Src kinases (Lyn, Fyn, c-Src, and Lck) bind Nef but with lower affinities (Arold et al., 1998; Karkkainen et al., 2006; Trible et al., 2006). Importantly, the disruption of proline-rich PxxP motif of Nef, an essential motif to bind the Src homology 3 (SH3) domain of Hck, was sufficient to protect Tg mice from the AIDS-like disease, and wild-type Nef-induced disease progression was significantly delayed in $Hck^{-/-}$ mice (Hanna et al., 2001), indicating that high affinity Nef-Hck binding in macrophages is at least in part responsible for disease development and progression. However, unresolved issue is how Nef-Hck binding followed by activation of Hck (Moarefi et al., 1997; Lerner and Smithgall, 2002) satisfactorily account for disease development and progression.

An important clue to the issue is that Nef predominantly localized to the Golgi apparatus (Greenberg et al., 1998; Drakesmith et al., 2005; Haller et al., 2007) and that Nef not only activated Hck but also induced skewed localization of Hck to the Golgi (Hung et al., 2007). The Golgi functions as a sorting hub and location of glycosylation for proteins, and several lines of evidence have revealed that Src kinases, shown to be involved in a wide array of intracellular signaling (reviewed in

Contract grant sponsor: Ministry of Education, Culture, Sports, Science and Technology of Japan.
Contract grant sponsor: Human Science Foundation, Japan.

*Correspondence to: Seiji Okada, Division of Hematopoiesis, Center for AIDS Research, Kumamoto University, Kumamoto 860-0811, Japan. E-mail: okadas@kumamoto-u.ac.jp

Received 17 February 2009; Accepted 11 June 2009

Published online in Wiley InterScience (www.interscience.wiley.com.), 7 July 2009.
DOI: 10.1002/jcp.21878

Lowell, 2004), also play a role in the regulation of the Golgi structure/function. First, a fraction of Src kinases, including Hck, is physiologically found at the Golgi (David-Pfeuty and Nouvian-Dooghe, 1990; Kaplan et al., 1992; Ley et al., 1994; Bijlmakers et al., 1997; van't Hof and Resh, 1997; Carreno et al., 2000; Kasahara et al., 2004). Second, fibroblasts lacking three ubiquitous Src kinases (c-Src/Yes/Fyn) exhibited an aberrant Golgi structure composed of collapsed stacks and bloated cisternae (Bard et al., 2003). Third, an increased protein load entering the *cis*-Golgi from the endoplasmic reticulum activated the Golgi-localized Src kinases, which in turn regulated overall protein trafficking activity in the secretory pathway (Pulvirenti et al., 2008). Importantly, the study by Pulvirenti et al. indicates that coordinated regulation of activity of the Golgi-localized Src kinases is crucial to maintain the Golgi function, which raises an intriguing possibility that Nef affects protein trafficking process and thereby macrophage phenotype/function through skewed Golgi-localization of active Hck.

Indeed, we recently identified an aberrant function of Nef, which was possibly due to the skewed Golgi-localization of active Hck. We previously found that Nef inhibited the signal of M-CSF, a primary cytokine for macrophages (Suzu et al., 2005), which was a possible trigger to worsen uncontrolled immune systems in patients, as M-CSF is essential to maintain macrophages at an anti-inflammatory state (reviewed in Hamilton, 2008). Of interest was the role of Hck in this inhibitory activity of Nef (Hiyoshi et al., 2008). Nef reduced cell surface expression of M-CSF receptor Fms in myeloid cells and macrophages, which was the direct cause of the inhibitory activity of Nef on M-CSF signal. Importantly, such reduced cell surface expression of Fms was reproduced in transfected 293 cells, but only in co-expression with Hck. More importantly, the reduced cell surface expression was due to the accumulation of an immature under-*N*-glycosylated Fms at the Golgi (hereinafter called Fms maturation arrest). However, constitutive-active Hck alone failed to induce such Fms maturation arrest. These results indicate that Nef inhibits M-CSF signal by arresting Fms *N*-glycosylation and trafficking at the Golgi and that such Fms maturation arrest was not caused just because of Hck activation. Thus, a most likely cause of Nef-induced Fms maturation arrest was skewed Golgi-localization of active Hck. However, this intriguing hypothesis should be carefully and directly tested, because it will not only help to clarify molecular basis of this novel function of Nef through Hck, but also provide an excellent example of disease-associated failure of the Golgi function regulation by the Golgi-localized Src kinases.

In this study, we therefore sought to definitely conclude that skewed Golgi-localization of active Hck was indeed the direct cause of Fms maturation arrest by Nef. To this end, we employed two different approaches. First, we prepared various Nef proteins and compared their abilities to induce skewed Golgi-localization of Hck, Hck activation and Fms maturation arrest. Second and importantly, we discovered a small-molecule non-kinase inhibitor that effectively blocked Nef-Hck binding and performed mechanistic analyses with the newly discovered compound.

Materials and Methods

Expression plasmids

For the expression in HEK293 cells (Invitrogen, Carlsbad, CA), human Fms- and human p56Hck cDNA cloned into pCDNA3.1 vector (Invitrogen) were used (Suzu et al., 2005; Hiyoshi et al., 2008). The constitutive-active Hck P2A mutant (Hiyoshi et al., 2008) was also used in selected experiments. The expression plasmid for human Lyn cloned in pME-puro vector was provided by Y. Yamanashi (Tokyo Medical and Dental University, Tokyo, Japan) and used in the pull-down assay with GST-Nef fusion proteins (see below). Nef cDNA derived from the NL43 or SF2 strain of HIV-1 was cloned into pRc/CMV-CD8 vector to express the extracellular/transmembrane regions of CD8-Nef fusion protein (Hiyoshi et al., 2008). NL43 Nef-M20A was prepared as described previously (Akari et al., 2000). NL43 Nef-AxxA and $-\Delta E$ mutant were provided by A. Adachi (University of Tokushima, Tokushima, Japan) and J.C. Guatelli (University of California, San Diego, CA), respectively. In this study, we prepared another NL43 Nef mutant (NL43 Nef-TR), by using QuikChange II Site-directed Mutagenesis Kits (Stratagene, La Jolla, CA). We also prepared Nef constructs expressing Nef-GFP fusion proteins (Ueno et al., 2008). For the expression of GST-Nef fusion proteins, fragments containing the entire coding sequences of the wild-type NL43 Nef, NL43 Nef-TR mutant, wild-type SF2 Nef, and SF2 Nef-AxxA mutant were subcloned into pGEX-6P-1 vector (GE Healthcare, Buckinghamshire, UK). SF2 Nef-AxxA mutant was prepared by using QuikChange II Site-directed Mutagenesis Kits (Stratagene). The nucleotide sequences of the coding region of all Nef constructs were verified by using BigDye Terminator v3.1 Cycle Sequencing Kit (Applied Biosystems, Foster City, CA) and ABI PRISM 3100 Genetic Analyzer (Applied Biosystems).

Chemicals

PP2 (Sigma, San Diego, CA) was used as the Src kinase inhibitor. UCS15A and its synthetic derivatives, 2b and 2c, were prepared as described (Oneyama et al., 2003). All these inhibitors were dissolved in dimethyl sulfoxide (DMSO; Wako, Osaka, Japan).

Western blotting

HEK293 cells were maintained with DME medium (Wako) supplemented with 10% fetal calf serum (FCS). The maturation of Fms proteins or the activation of Hck was analyzed by the transient expression assay with the cells followed by Western blotting as described previously (Suzu et al., 2005; Hiyoshi et al., 2008). In brief, cells grown on a 12-well tissue culture plate were transfected with plasmid for Fms (0.4 μg), Nef (0.8 μg), or Hck (0.4 μg) in the combinations indicated using LipofectAMINE2000 reagent (Invitrogen), unless otherwise stated. Total amounts of plasmids were normalized with the empty vectors. After 6 h, culture medium was replaced with complete medium and the transfected cells were cultured for an additional 42 h. In selected experiments, chemicals such as PP2 and 2c were added to the culture at the same time of changing medium. Total cell lysates were prepared essentially as described (Suzu et al., 2000). Primary antibodies used for Western blotting were as follows: anti-Fms (C-20; Santa Cruz Biotechnology, Santa Cruz, CA), anti-CD8 (H-160; Santa Cruz), anti-GFP (FL; Santa Cruz), anti-Hck (clone 18; Transduction Laboratories, Lexington, KY), anti-Hck phosphorylated at tyrosine 411 (Hck-pTyr^{411}; Santa Cruz), anti-phosphotyrosine (PY99; Santa Cruz), and anti-ERK1/2 (K-23; Santa Cruz). The relative intensity of bands on scanned gel images was quantified using NIH Image software, and the Fms maturation arrest or Hck activation is also shown graphically on an arbitrary unit. The relative intensity of bands on Hck-pTyr^{411} blots was quantified and the degree of Hck activation was expressed as a fold-increase relative to the control. For Fms maturation arrest, we calculated the percentage of immature under-*N*-glycosylated Fms of total Fms protein amount, and compared the percentages among samples.

Immunofluorescence

The signal of Nef-GFP was directly visualized with a BZ-8000 fluorescent microscope (Keyence, Osaka, Japan) equipped with Plan-Fluor ELWD 20x/0.45 objective lenses (Nikon, Tokyo, Japan) (Hiyoshi et al., 2008). To detect active Hck, cells were fixed in 2% paraformaldehyde, permeabilized with ethanol, and stained with goat anti-active Hck antibodies (Santa Cruz). Secondary antibodies were anti-goat IgG-AlexaFluo488 (Molecular Probes, Eugene, OR). Nuclei were stained with DAPI (Molecular Probes), and

fluorescent signals were visualized as above. Image processing was performed using BZ-analyzer (Keyence) and Adobe Photoshop Software (Adobe Systems, San Jose, CA).

GST pull-down

The control GST or GST-Nef fusion proteins (wild-type NL43 Nef, NL43 Nef-TR, wild-type SF2 Nef, and SF2 Nef-AxxA) cloned in pGEX-6P-1 vector was expressed in *E. coli* BL21 cells (GE Healthcare). Cells were grown in LB media containing 50 μg/ml ampicillin followed by induction with 1 μM IPTG. The expression-induced cells were harvested and lysed with BugBuster Protein Extraction Reagent containing 1 U/ml rLysozyme and 25 U/ml Benzonaze Nuclease (Novagen, Madison, WI). The cleared lysates were then incubated with GST-Bind Resin (Novagen). After extensive washing with GST Bind/Wash Buffer (Novagen), the resin was incubated with the total cell lysates of HEK293 cells transfected with the expression plasmid for Hck or Lyn. In a selected experiment, 2c was added to the mixtures. After extensive re-washing, the resin was boiled with SDS–PAGE sample buffer and elutes were analyzed for the presence of Hck or Lyn by western blotting. Primary antibodies used were as follows (both from Transduction Laboratories): anti-Hck (clone 18) and anti-Lyn (clone 42). In a selected experiment, we also used GST proteins fused to the SH3 domain of Hck (Paliwal et al., 2007), which was provided by G. Swarup (Center for Cellular and Molecular Biology, Hyderabad, India).

Subcellular fractionation

The subcellular fractionation on sucrose gradients was performed exactly as reported (Matsuda et al., 2006). In brief, cells were

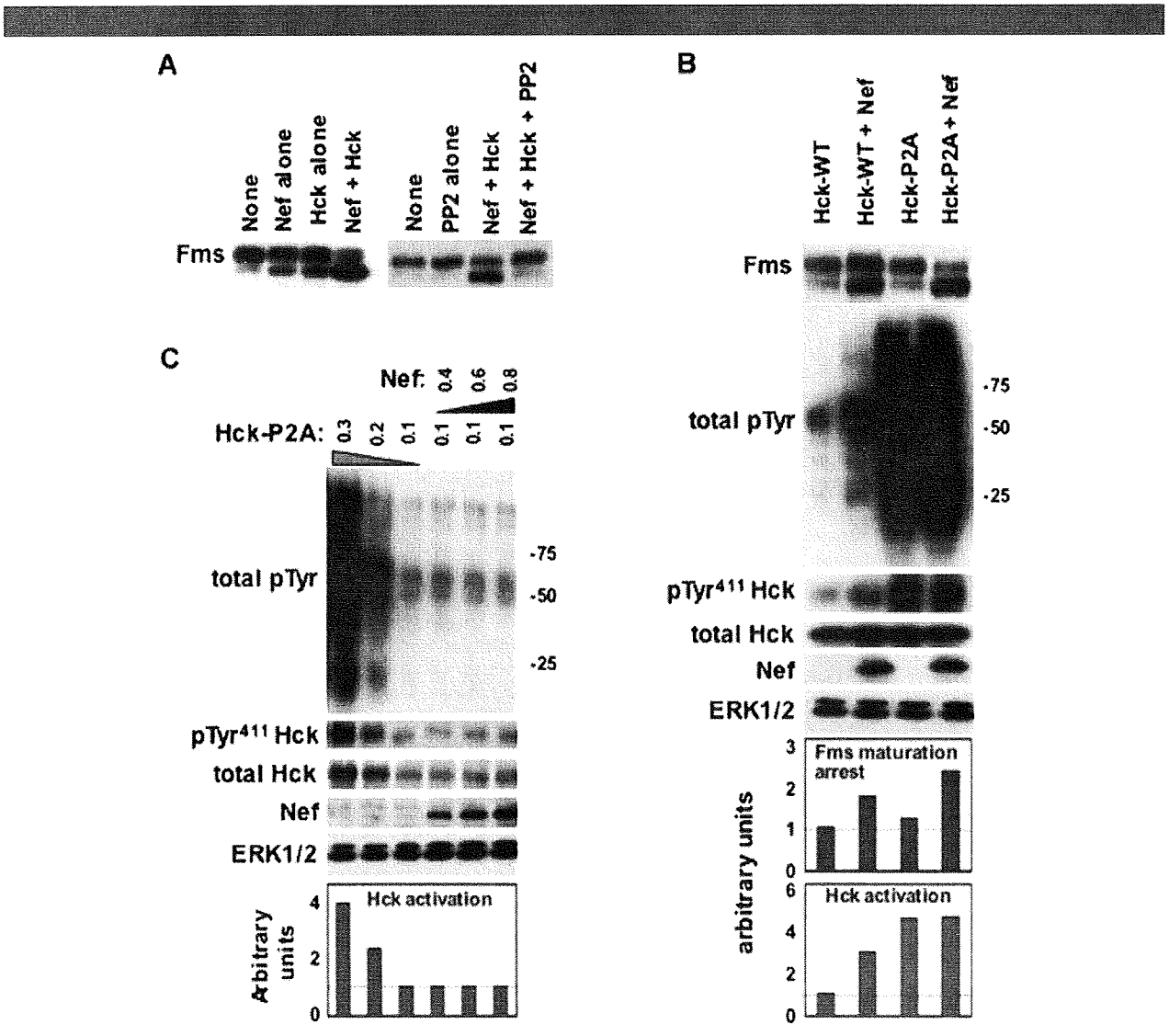

Fig. 1. Nef/Hck-induced Fms mturation arrest. A: HEK293 cells were transfected with Fms plamid alone (None) or co-transfected with the plasmids for NL43 Nef and/or wild-type Hck as indicated. In the right blot, PP2 was added to selected wells at a final concentration of 10 μM after the transfection, Total cell lysates were subjected to Fms Western blotting. B: Cells were transfected with Fms plasmid alone (None) or in combination with the plasmids for Nef (NL43) and Hck (WT or constitutive-active P2A), as indicated. These cells were then analyzed for the expression of Fms, tyrosine-phosphorylated proteins (total pTyr), active-Hck (pTyr^{411}Hck), total Hck, CD8-Nef (Nef), or ERK by Western blotting. The ERK blot is a loading control. The quantified Fms maturation arrest and Hck activation are shown in the bar graphs. C: Cells were transfected with varying amounts (μg) of Hck-P2A and NL43 Nef plasmids as indicated, and analyzed as in (B). The quantified Hck activation is shown in the bar graphs. [Color figure can be viewed in the online issue, which is available at www.interscience.wiley.com.]

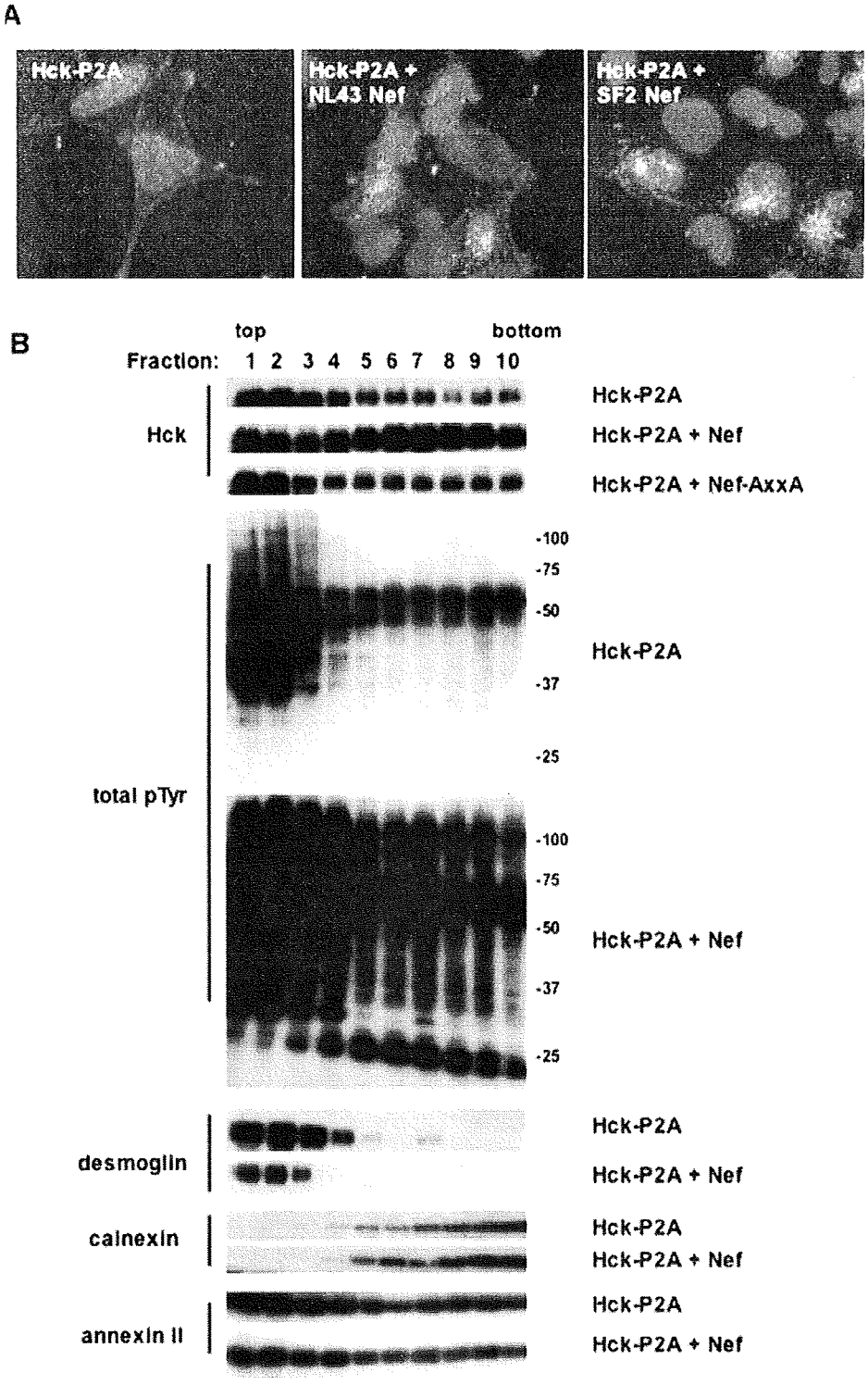

Fig. 2. Skewed Golgi-localization of Hck by Nef. A: HEK293 cells were transfected with Hck-P2A plasmid alone, or co-transfected with NL43 Nef or SF2 Nef plasmid. Cells were stained with antibody specific for active Hck (green) and DAPI (blue). B: Cells were transfected with Hck-P2A alone, or co-transfected with NL43 Nef. Then, cells were subjected to subcellular fractionation on sucrose gradients and Western blotting with antibodies against Hck, phosphotyrosine (pTyr), desmoglein, calnexin, or annexin II. [Color figure can be viewed in the online issue, which is available at www.interscience.wiley.com.]

swollen in hypotonic buffer containing protease inhibitors followed by homogenization. Then, the post-nuclear supernatants were fractionated by ultracentrifugation on discontinuous sucrose gradients. All steps were carried out on ice. The fractions obtained were subjected to Western blotting with antibodies to Hck (clone 18; Transduction Laboratories), desmoglein (clone 62; Transduction Laboratories), annexin II (C-10; Santa Cruz), or calnexin (H-70; Santa Cruz).

Flow cytometry

Human myeloid TF-1-fms cells expressing Nef-ER fusion protein were maintained as described previously (Suzu et al., 2005; Hiyoshi et al., 2008). To activate the Nef-ER fusion protein, we used the estrogen analog 4-HT (Sigma) at a final concentration of 0.1 μM. The cells were stained with PE-labeled anti-Fms antibodies (Santa Cruz), and the level of cell surface Fms was analyzed by flow cytometry on a FACS Calibur using Cell Quest software (Becton Dickinson, Mountain View, CA).

Results

Analyses with Src kinase inhibitor and Hck mutant

As reported, Nef induces Fms maturation arrest when co-expressed with Hck in HEK293 cells (Fig. 1A). HEK293 cells do not express Hck endogenously, and the upper and lower band was the fully *N*-glycosylated and under-*N*-glycosylated Fms, respectively (Hiyoshi et al., 2008). The low molecular weight Fms was sensitive to Endo-H (Endo-β-*N*-acetylglucosaminindase H), which selectively cleaves high-mannose type oligosaccharide, and their increase was clearly associated with the intense staining of Fms mainly at

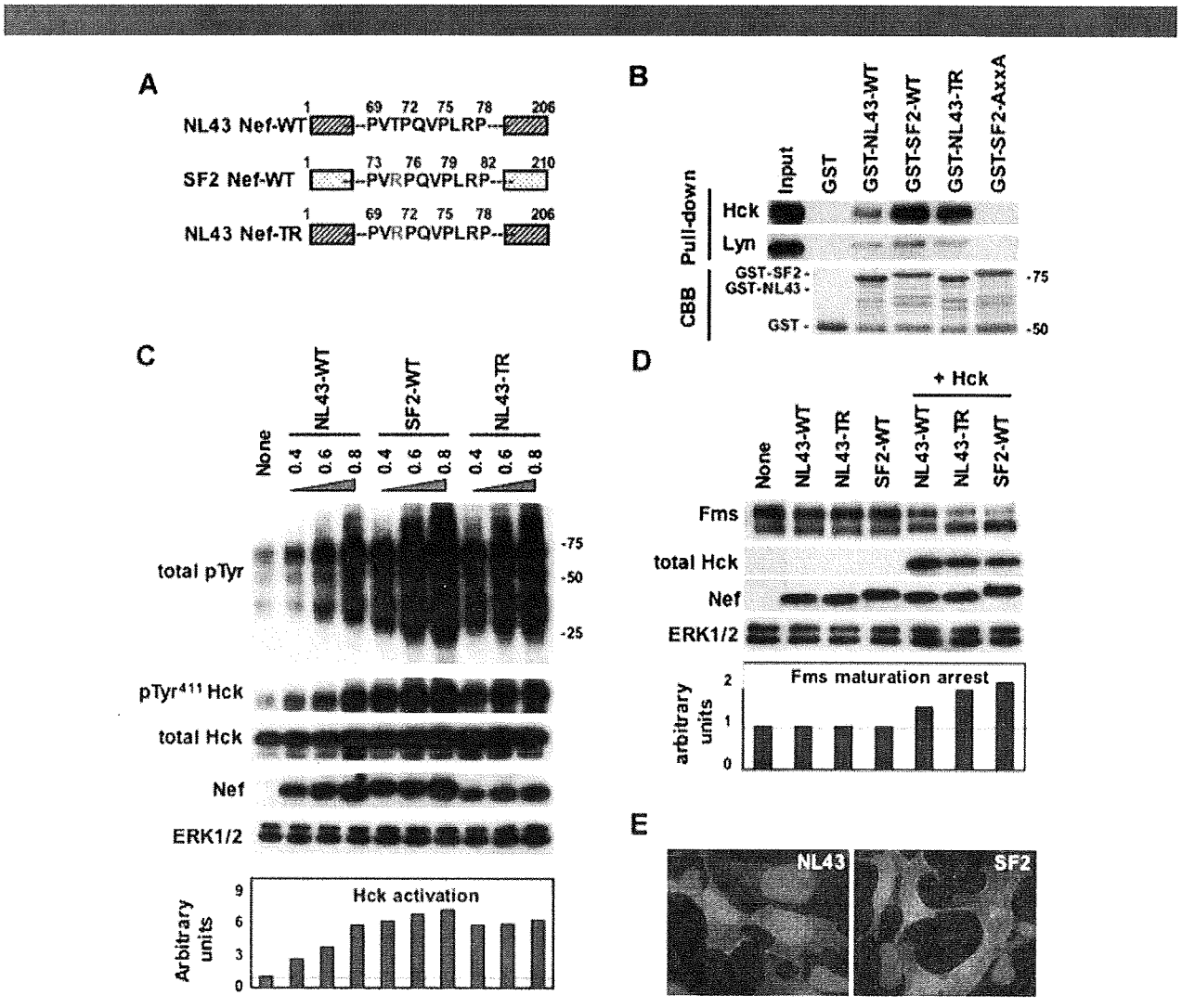

Fig. 3. Abilities of different Nef alleles to bind/activate Hck and to induce Fms maturation arrest. A: The NL43 Nef, SF2 Nef, and NL43 Nef-TR mutant used are schematically shown. B: The resins, to which the control GST or indicated GST-Nef proteins were bound, were incubated with the lysates of HEK293 cells expressing Hck or Lyn. The amount of Hck or Lyn bound to the resins was determined by Western blotting (Pull-down). The amount of GST and GST-Nef fusion proteins bound to the resins was verified by the elution from the resins followed by SDS–PAGE/Coomassie brilliant blue (CBB) staining. C: HEK293 cells were co-transfected with the wild-type Hck and indicated Nef alleles. The amounts of Nef plasmids used are shown (0.4, 0.6, or 0.8 μg/well). Total cell lysates were subjected to Western blotting with antibodies against phosphotyrosine (total pTyr), active-Hck (pTyr^{411}Hck), total Hck, CD8-Nef (Nef), or ERK by Western blotting. The quantified Hck activation is shown in the bar graph. D: Cells were transfected with Fms plasmid alone (None) or in combination with the plasmids for Nef and Hck, as indicated. Western blotting was done as in (C). E: Cells were transfected with indicated GFP-Nef plasmid (green). Nuclei were stained with DAPI (blue). [Color figure can be viewed in the online issue, which is available at www.interscience.wiley.com.]

the perinuclear region, which overlapped well with the signal of GM130 or Vti1a, the markers for the Golgi (Hiyoshi et al., 2008). These results strongly suggested that the low molecular weight Fms was the immature under-*N*-glycosylated form. The increase of the lower molecular weight species was obvious in the cells co-expressing Nef and Hck (Fig. 1A, left blot), and this Fms maturation arrest was blocked by a Src kinase inhibitor PP2 (Fig. 1A, right blot). However, the expression of a constitutive-active Hck mutant (Hck-P2A; Lerner and Smithgall, 2002) was not sufficient to induce Fms maturation arrest when expressed alone (Fig. 1B, Fms blot), despite its strong kinase activity (total pTyr and $pTyr^{411}$ Hck blots). In this study, we monitored kinase activity of Hck by overall protein tyrosine-phosphorylation (total pTyr) and auto-phosphorylation of Hck ($pTyr^{411}$ Hck) (reviewed in Korade-Mirnics and Corey, 2000). Nonetheless, Hck-P2A/Nef co-expression induced more severe Fms maturation arrest than wild-type Hck/Nef co-expression (Fig. 1B), and Nef did not enhance the kinase activity of Hck-P2A (Fig. 1C), confirming our previous finding that Hck activation was necessary but not sufficient for Nef-induced Fms maturation arrest.

Analyses with different Nef alleles and their mutants

In this study, we first found that Nef derived from SF2 strain of HIV-1 induced more severe Golgi-localization of Hck-P2A than Nef derived from NL43 strain. Hck-P2A signal at the plasma membrane was still observed in some NL43 Nef-transfected cells, whereas such signal was not observed in SF2 Nef-transfected cells (Fig. 2A). The Nef-induced skewed Golgi-localization of Hck-2PA was confirmed by a quantitative analysis, that is, subcellular fractionation on sucrose gradients. Based on a previous report (Matsuda et al., 2006), we used desmoglein, annexin II and calnexin as marker proteins for the plasma membrane, both the plasma membrane and the Golgi, and the endoplasmic reticulum, respectively. As shown (Fig. 2B), the plasma membrane was recovered in light fractions whereas the Golgi and the endoplasmic reticulum were recovered in heavy fractions, and the peak of Hck-P2A shifted to heavy fractions by the co-expression with NL43 Nef but not a Nef-AxxA mutant defective in the binding to Hck (Saksela et al., 1995). The peak shift was also associated with the appearance of many tyrosine-phosphorylated proteins in these fractions (Fig. 2B).

Both NL43 Nef and SF2 Nef had intact PxxP motif (Fig. 3A), but SF2 Nef showed much higher affinity to Hck than NL43 Nef (Fig. 3B). In the control experiments, we confirmed that the binding of both Nef to Lyn remained low and the PxxP motif-disrupted SF2 Nef mutant (AxxA) bound neither Hck nor Lyn. Reflecting the higher affinity to Hck, SF2 Nef induced stronger Hck activation (Fig. 3C) and more severe Fms maturation arrest (Fig. 3D). As expected, even SF2 Nef failed to induce Fms maturation arrest when co-expressed with Lyn (data not shown). However, SF2 Nef and NL43 Nef showed no obvious change in the pattern of predominant Golgi-localization (Fig. 3E). It was therefore likely that SF2 Nef bound Hck at

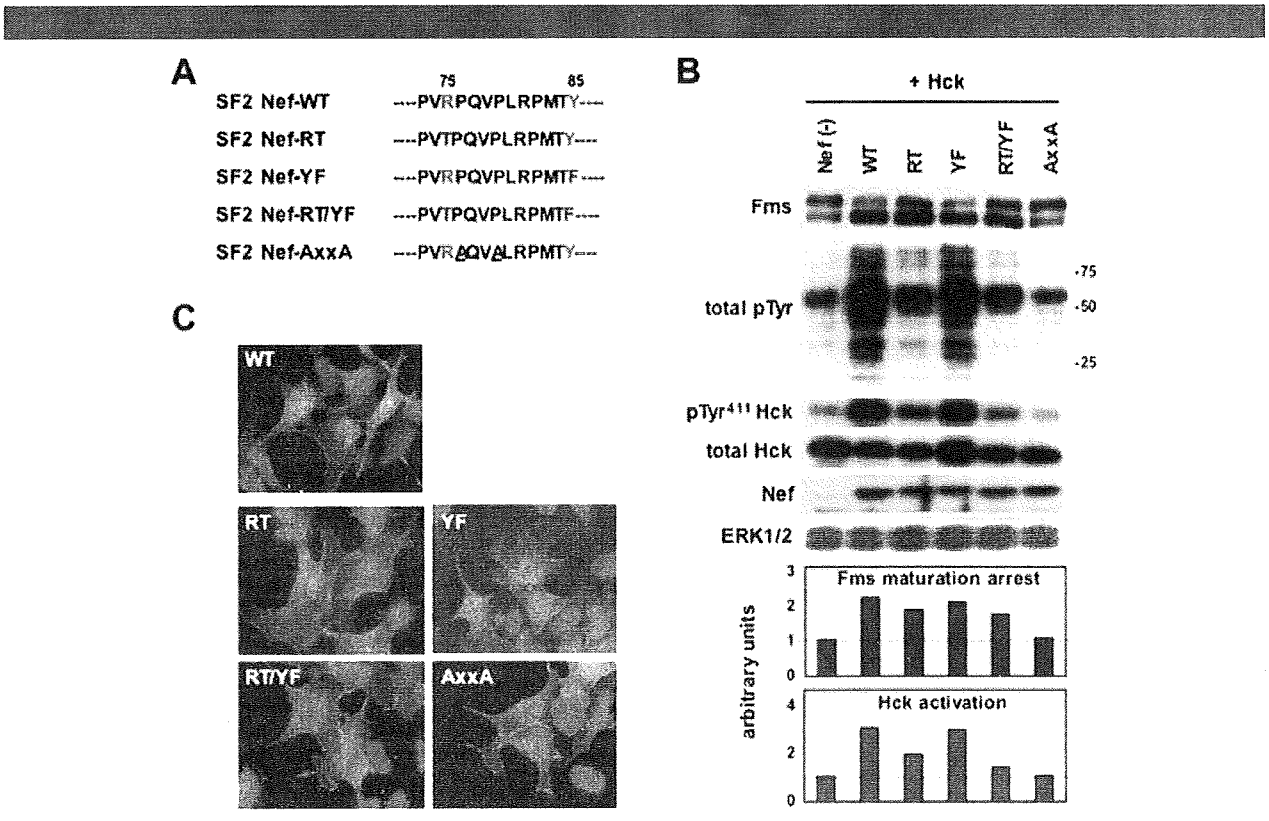

Fig. 4. Abilities of SF2 Nef mutants to activate Hck and to induce Fms maturation arrest. A: The SF2 Nef mutants used (RT, YF, RT/YF, and AxxA) are schematically shown. B: HEK293 cells were transfected with Fms plasmid alone (None) or in combination with the plasmids for Nef and Hck, as indicated. These cells were then analyzed for the expression of Fms, phosphotyrosine (total pTyr), active-Hck ($pTyr^{411}$Hck), total Hck, GFP-Nef (Nef), or ERK by Western blotting. The quantified Fms maturation arrest and Hck activation are shown in the bar graphs. C: Cells were transfected with indicated GFP-Nef plasmid (green). Nuclei were stained with DAPI (blue). [Color figure can be viewed in the online issue, which is available at www.interscience.wiley.com.]

the Golgi with higher affinity and thereby induced stronger Hck activation and more severe Fms maturation arrest.

There was a single amino acid difference within the PxxP motif, Thr^{71} in NL43 Nef and Arg^{75} in SF2 Nef (Fig. 3A). We found that an NL43 Nef with $Thr^{71}Arg$ substitution (NL43 Nef-TR) showed higher affinity to Hck than wild-type NL43 Nef (Fig. 3B), and induced stronger Hck activation (Fig. 3C) and more severe Fms maturation arrest (Fig. 3D) than wild-type NL43 Nef. We also performed a complementary experiment with SF2 Nef mutants (Fig. 4A; Ueno et al., 2008). As a result, we found that mutants with $Arg^{75}Thr$ substitution (SF2 Nef-RT and SF2-RT/YF) induced moderate Hck activation/Fms maturation arrest (Fig. 4B). However, both showed no obvious change in the pattern of predominant Golgi-localization (Fig. 4C). These results indicated that the single amino acid difference (Thr to Arg) within the PxxP motif governed the higher ability of SF2 Nef to induce Golgi-localization and activation of Hck, and Fms maturation arrest.

Although PxxP motif is essential for Nef to bind Hck, a recent study showed that an acidic region of Nef facilitated Nef-Hck binding at the Golgi (Hung et al., 2007). Although an NL43 Nef mutant lacking this region (ΔE; Fig. 5A) bound GST-Hck SH3 fusion proteins as with wild-type NL43 Nef (Fig. 5B), ΔE mutant was indeed less active than wild-type in transfected HEK293 cells, that is, in both Hck and activation Fms maturation arrest (Fig. 5C). Another mutant (M20; Fig. 5A), which was defective in the down-regulation of MHC I, another hallmark function of Nef (Akari et al., 2000), retained the ability to induce Hck activation and Fms maturation arrest (Fig. 5C). Both ΔE and M20A mutants showed no obvious change in the pattern of predominant Golgi-localization (Fig. 5C). The result further supported the idea that stronger Hck activation, which took place at the Golgi, induced severe Fms maturation arrest.

Analyses with a newly discovered Nef-Hck binding blocker

To directly show that the Golgi-localization of active Hck determines Nef-induced Fms maturation arrest, we sought to discover Nef-Hck binding blockers. In this study, we focused on UCS15A and its analogs 2b and 2c (Fig. 6A), because these small-molecule compounds were shown to block several proline-rich motif-SH3 domain binding such as Sam68-Fyn binding (Oneyama et al., 2003) and AMAP1-cortactin binding (Hashimoto et al., 2006). As they have not been used before for HIV-1 studies, we tested their capability to block Nef-Hck binding by the GST pull-down assay. As shown (Fig. 6B), all compounds blocked the binding of Hck to NL43 Nef or NL43 Nef-TR mutant (more potent than the wild-type, see Fig. 3), in a dose-dependent manner. Like the case of Sam68-Fyn binding (Oneyama et al., 2003), 2c was the most effective in blocking Nef-Hck binding (Fig. 6B), and showed no obvious toxicity to HEK293 cells (Fig. 6C). As shown (Fig. 6D), 2c indeed inhibited

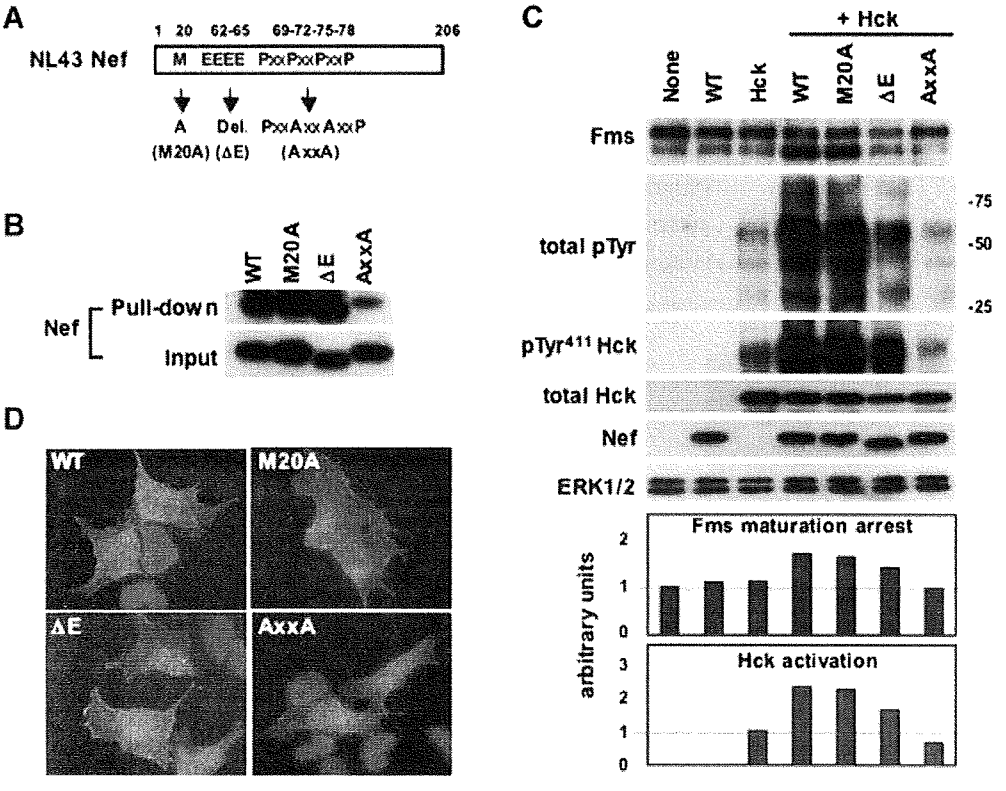

Fig. 5. Abilities of NL43 Nef mutants to activate Hck and to induce Fms maturation arrest. A: The NL43 Nef mutants used (M20A, ΔE, and AxxA) are schematically shown. B: The resin, to which GST-Hck SH3 fusion proteins were bound, were incubated with the lysates of HEK293 cells expressing the indicated Nef proteins. The amount of Nef proteins in the lysates (Input) or bound to the resins (Pull-down) was verified by Western blotting. C: HEK293 cells were transfected with Fms plasmid alone (None) or in combination with the plasmids for Nef and Hck, as indicated. These cells were then analyzed for the expression of Fms, phosphotyrosine (total pTyr), active-Hck ($pTyr^{411}$ Hck), total Hck, CD8-Nef (Nef), or ERK by Western blotting. The quantified Fms maturation arrest and Hck activation are shown in the bar graphs. D: Cells were transfected with indicated GFP-Nef (green). Nuclei were stained with DAPI (blue). [Color figure can be viewed in the online issue, which is available at www.interscience.wiley.com.]

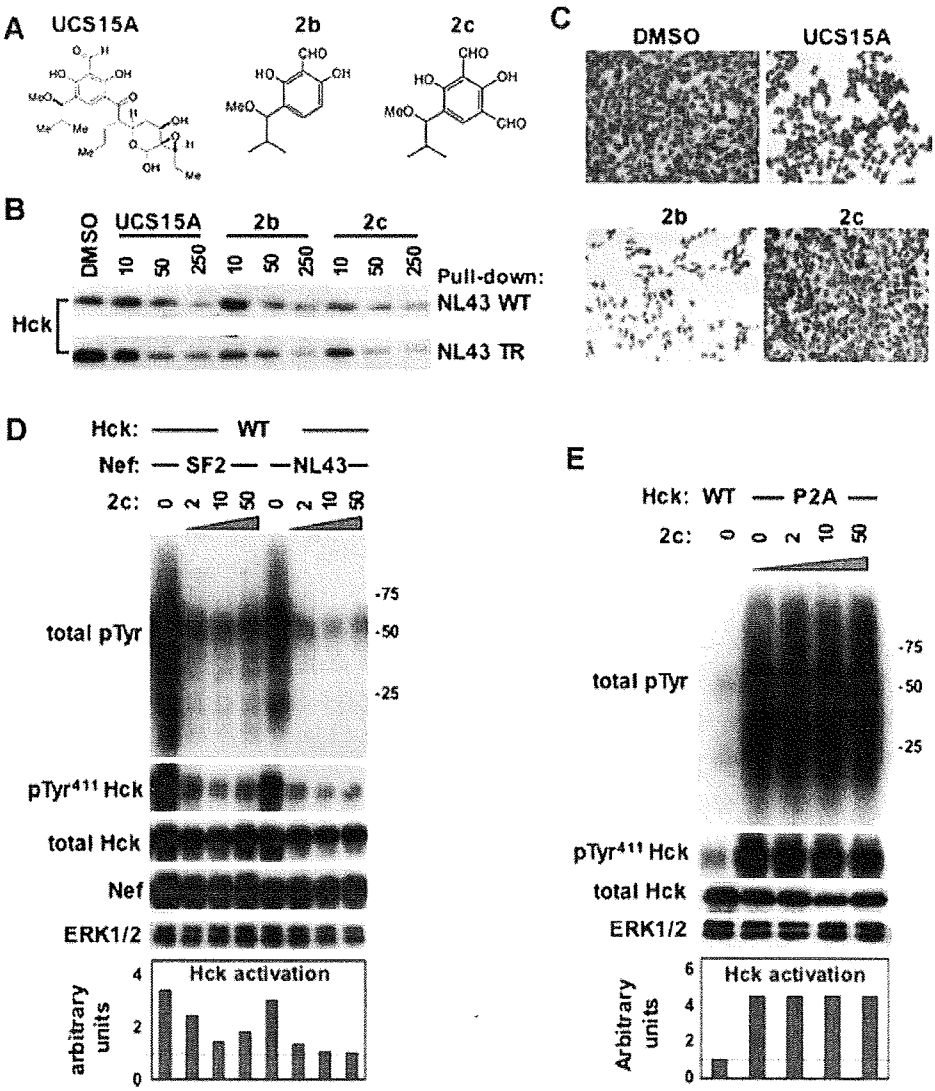

Fig. 6. Capability of 2c to block Nef-Hck binding and Nef-induced Hck activation. A: Chemical structures of UCS15A, 2b, and 2c are shown. B: The resins, to which GST-Nef (NL43 wild-type or TR mutant, see Fig. 2A) proteins were bound, were incubated with the lysates of Hck-expressing HEK293 cells in the absence (DMSO) or presence of the indicated concentration (0, 10, 50, or 250 μM) of UCS15A, 2b, or 2c. The amount of Hck proteins bound to the resins was determined by Western blotting. C: HEK293 cells were cultured in the absence (DMSO) or presence of 50 μM of UCS15A, 2b, or 2c for 2 days, and subjected to Wright-Giemsa staining. D: Cells were co-transfected with Hck-WT and indicated Nef alleles (SF2 or NL43), and cultured in the presence of increasing concentrations (μM) of 2c. These cells were then analyzed for the expression of tyrosine-phosphorylated proteins (total pTyr), active-Hck (pTyr^{411}Hck), total Hck, CD8-Nef (Nef), or ERK by Western blotting. The quantified Hck activation is shown in the bar graphs. E: Cells were transfected with Hck-WT or Hck-P2A, and cultured in the presence of increasing concentrations (μM) of 2c. These cells were analyzed as in (D). [Color figure can be viewed in the online issue, which is available at www.interscience.wiley.com.]

Hck activation by NL43 Nef and more potent SF2 Nef (see Fig. 3). Importantly, 2c had little inhibitory effect on kinase activity of the constitutive-active Hck P2A mutant, even when used at a concentration as high as 50 μM (Fig. 6E). These results indicated that 2c was not a kinase inhibitor but inhibited Nef-induced Hck activation by blocking Nef-Hck binding.

This unique feature of 2c prompted us to examine whether 2c blocks Nef/Hck-induced Fms maturation arrest and Nef-induced skewed Golgi-localization of Hck. As shown (Fig. 7A), 2c completely blocked Fms maturation arrest induced by Nef and wild-type Hck as expected. However, of particular importance was that 2c also completely blocked severe Fms maturation arrest induced by Nef and the constitutive-active Hck P2A (Fig. 7B). Because 2c had little inhibitory effect on kinase activity of Hck-P2A (see Fig. 6E), these results strongly supported that the presence of Hck-P2A at the Golgi caused by its binding with Nef (see Fig. 2) was a direct cause of severe Fms maturation arrest. We therefore sought to verify that 2c indeed blocked Nef-induced skewed Golgi-localization of Hck-P2A. To this end, we employed the quantitative analysis, that is, subcellular fractionation on sucrose gradients (see Fig. 2B). The peak of Hck-P2A shifted to heavier fractions by the co-expression with Nef, and such change in the intracellular localization of Hck-P2A was restored to normal by the addition of 2c (Fig. 7C). We also tested whether 2c blocked Nef-induced Fms abnormality in another culture system. We previously showed that the cell surface expression of Fms was impaired in human myeloid TF-1-fms cells expressing a conditionally active

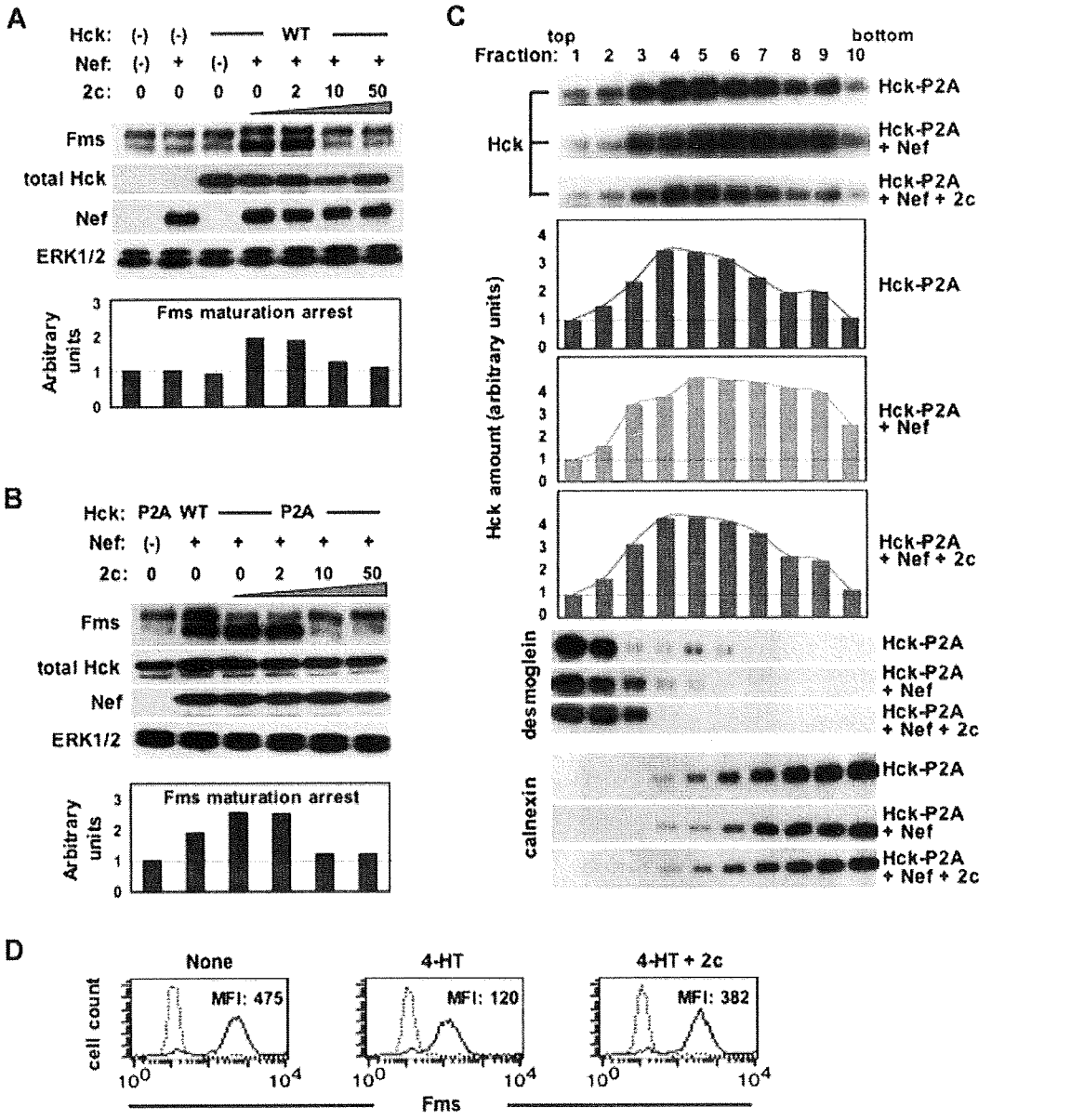

Fig. 7. Capability of 2c to block Fms maturation arrest and skewed Golgi-localization of Hck. A: HEK293 cells were transfected with the plasmids (Fms, NL43 Nef, and Hck-WT) in combination indicated, and cultured in the presence of increasing concentrations (μM) of 2c. These cells were then analyzed for the expression of Fms, total Hck, CD8-Nef (Nef), or ERK by Western blotting. The quantified Fms maturation arrest is shown in the bar graphs. B: Cells were transfected with the plasmids (Fms, NL43 Nef, Hck-WT, and Hck-P2A) in combination indicated, and cultured in the presence of increasing concentrations (μM) of 2c. These cells were then analyzed as in A. C: Cells were transfected with Hck-P2A alone (top), or co-transfected with NL43 Nef (middle). 2c was added to a final concentration of 50 μM to selected wells (bottom). Then, cells were subjected to subcellular fractionation on sucrose gradients and Hck Western blotting. The quantified Hck amounts are shown in the bar graph. The fractions were also analyzed for the amount of desmoglein and calnexin. D: TF-1-fms-Nef-ER cells cultured with M-CSF-free media in the absence (left) or presence of 0.1 μM 4-HT (middle), or the co-presence of 0.1 μM 4-HT and 50 μM 2c (right) for 12 h. The expression of Fms on the surface of treated cells was analyzed by flow cytometry with PE-labeled anti-Fms. The mean fluorescence intensity (MFI) of Fms expression is indicated. [Color figure can be viewed in the online issue, which is available at www.interscience.wiley.com.]

Nef-ER fusion protein when the Nef-ER in the cells was activated by the estrogen analog 4-HT (Hiyoshi et al., 2008). This impaired cell surface Fms expression was highly likely due to intracellular Fms maturation arrest (Hiyoshi et al., 2008). Finally, we found that the Fms down-regulation in Nef-active TF-1-fms-Nef-ER cells was also restored to normal by the addition of 2c (Fig. 7D). All taken together, our present study clearly demonstrated that skewed Golgi-localization of active Hck induced by Nef was indeed the direct cause of Fms maturation arrest.

Discussion

M-CSF is a cytokine essential not only for the survival of macrophages but also for the maintenance of macrophages at an

anti-inflammatory state (reviewed in Chitu and Stanley, 2006; Hamilton, 2008). Thus, the inhibitory effect of Nef on M-CSF signal through Fms maturation arrest at the Golgi is a possible trigger to worsen uncontrolled immune systems in patients (Suzu et al., 2005; Hiyoshi et al., 2008). In this study, we therefore sought to define molecular basis of this important function of Nef, by using different Nef alleles, various Nef mutants, constitutive-active Hck mutant, and Nef-Hck binding blocker 2c. The study with various Nef proteins supported the idea that high affinity Nef-Hck binding and subsequent stronger Hck activation, both of which took place mainly at the Golgi, determined Fms maturation arrest at the Golgi (Figs. 2–5). Moreover, the study with 2c enabled us to conclude that skewed Golgi-localization of active Hck by Nef was indeed the direct cause of Fms maturation arrest (Figs. 6 and 7). By analogy with the Sam68-Fyn binding inhibition (Oneyama et al., 2003), the inhibitory effect of 2c on Nef-Hck binding was supposed to be mediated by its interaction with Nef PxxP motif.

As mentioned earlier, it has been known for a long time that most members of Src kinases including Hck localize to the Golgi as well as to the plasma membrane. For example, it was shown that newly synthesized Lyn initially localized and accumulated to the Golgi, and then moved toward the plasma membrane (Kasahara et al., 2004). Importantly, Pulvirenti et al. (2008) recently revealed that coordinated regulation of activity of the Golgi-localized Src kinases is crucial to maintain intra-Golgi trafficking of proteins. Our present finding that skewed Golgi-localization of active Hck leads to Fms maturation arrest at the Golgi is in line with the new concept. It appears that long-lasting and dys-regulated activation of the Golgi-localized Src kinases disturbs glycosylation and/or trafficking of proteins, exemplified by Fms maturation arrest. Indeed, N-Src, a c-Src isoform with a higher basal tyrosine kinase activity (Brugge et al., 1985), showed more obvious perinuclear localization than the constitutive-active Hck-P2A and induced Fms maturation arrest even in the absence of Nef (unpublished result). Moreover, Mitina et al. (2007) reported that over-expression of an active form of Hck disturbed *N*-glycosylation of another cytokine receptor Flt3 even in the absence of Nef. These results may further support the idea that long-lasting and dys-regulated activation of the Golgi-localized Src kinases per se affects protein glycosylation and/or trafficking at the Golgi. Anyhow, our system with Nef provides a useful model to elucidate how Src kinases regulate the Golgi structure/function. It will be important to identify which Golgi proteins are phosphorylated directly or indirectly by Hck activated at the Golgi and to clarify how such phosphorylation cascade leads to Nef-induced Fms maturation arrest.

Nef has been shown to affect protein trafficking and a well-characterized target is major histocompatibility complex class I (MHC I). Nef reduced the cell surface expression of MHC I, which diminishes the recognition of infected cells by cytotoxic T cells (reviewed in Fackler and Baur, 2002; Peterlin and Trono, 2003). However, it is still in intense debate whether Nef requires SH3 domain-containing proteins such as Hck to reduce the cell surface level of MHC I (Schwartz et al., 1996; Greenberg et al., 1998; Mangasarian et al., 1999; Akari et al., 2000; Chang et al., 2001; Roeth and Collins, 2006; Hung et al., 2007; Atkins et al., 2008). In this regard, Fms is not the direct target of Nef. However, as shown, Nef disturbed the cell surface expression of Fms, which is triggered by skewed Golgi-localization of active Hck. Moreover, it was shown that Nef disturbed the cell surface expression of another macrophage-specific protein HFE, an iron homeostasis regulator, which was blocked by a dominant-negative Hck (Drakesmith et al., 2005). Although whether the reduced cell surface level of HFE by Nef relates to skewed Golgi-localization of active Hck is unclear, it is conceivable that Nef acquires an additional machinery to manipulate protein trafficking in macrophages by exploiting the Golgi-localized Hck. Of interest, the *N*-glycosylation of Flt3, which is structurally related to Fms, was also impaired in Nef/Hck-expressing HEK293 cells, but the degree of maturation arrest of Flt3 was quite weak when compared to that of Fms (data not shown). The finding may imply that Fms maturation arrest is not necessarily due to the general disruption in the Golgi structure or function. Future studies, in which we determine to what extent overall protein *N*-glycosylation and trafficking are affected by Nef-Hck binding, will further clarify pathological significance of the molecular binding in macrophages. The newly discovered Nef-Hck binding blocker 2c will be useful in such studies and may provide a strategy to complement current anti-HIV-1 therapy for better treatment outcomes.

In this study, we showed that SF2 Nef had much higher affinity to Hck than NL43 Nef and thereby induced stronger Hck activation/severe Golgi-localization of Hck (Figs. 2 and 3) and that the single amino acid difference (Thr^{71} in NL43 Nef and Arg^{75} in SF2 Nef) within PxxP motif largely governs the higher ability of SF2 Nef (Figs. 3 and 4). This difference might reflect that the $Thr^{71}Arg$ substitution in NL43 Nef (NL43 Nef-TR, see Fig. 3) altered the flexibility of a loop containing the PxxP motif (Fackler et al., 2001). Importantly, for reasons not clearly understood, NL43 Nef-TR was more pathogenic in HIV-1 Tg mice than wild-type NL43 Nef and the pathogenicity of SF2 Nef in Tg mice was evident despite very low levels of expression (Priceputu et al., 2007). It is therefore possible that more severe Golgi-localization of active Hck followed by perturbed *N*-glycosylation and trafficking of proteins including Fms account for the high pathogenicity of SF2 Nef in Tg mice.

In summary, our present study clearly demonstrated that skewed Golgi-localization of active Hck was the direct cause of Fms maturation arrest by Nef. Our findings establishes an intriguing link between the pathogenesis of HIV-1 Nef and the newly emerging concept that the Golgi-localized Src kinases regulate the Golgi function. The identification of Golgi proteins phosphorylated by the Golgi-localized active Hck will provide novel insights into molecular mechanisms by which Nef functions as an HIV-1 pathogenetic factor through Hck and the Gogi-localized Src kinases regulate the Golgi function.

Acknowledgments

We thank Dr. G. Thomas (Vollum Institute) for critical reading of the manuscript. We thank Ms. Y. Endo and Ms. I. Suzu for experimental assistance.

Literature Cited

Akari H, Arold S, Fukumori T, Okazaki T, Strebel K, Adachi A. 2000. Nef-induced major histocompatibility complex class I down-regulation is functionally dissociated from its virion incorporation, enhancement of viral infectivity, and CD4 down-regulation. J Virol 74:2907–2912.

Arold S, O'Brien R, Franken P, Strub MP, Hoh F, Dumas C, Ladbury JE. 1998. RT loop flexibility enhances the specificity of Src family SH3 domains for HIV-1 Nef. Biochemistry 37:14683–14691.

Atkins KM, Thomas L, Youker RT, Harriff MJ, Pissani F, You H, Thomas G. 2008. HIV-1 Nef binds PACS-2 to assemble a multikinase cascade that triggers major histocompatibility complex class I (MHC-I) down-regulation: Analysis using short interfering RNA and knock-out mice. J Biol Chem 283:11772–11784.

Bard F, Mazelin L, Pechoux-Longin C, Malhotra V, Jurdic P. 2003. Src regulates Golgi structure and KDEL receptor-dependent retrograde transport to the endoplasmic reticulum. J Biol Chem 278:46601–46606.

Bijlmakers MJ, Isobe-Nakamura M, Ruddock LJ, Marsh M. 1997. Intrinsic signals in the unique domain target p56lck to the plasma membrane independently of CD4. J Cell Biol 137:1029–1040.

Brugge JS, Cotton PC, Queral AE, Barrett JN, Nonner D, Keane RW. 1985. Neurones express high lenels of a structurally modified, activated form of pp60c-src. Nature 316:554–557.

Carreno S, Gouzè ME, Schaak S, Emorine LJ, Maridonneau-Parini I. 2000. Lack of palmitoylation redirects $p59^{Hck}$ from the plasma membrane to $p61^{Hck}$-positive lysosomes. J Biol Chem 275:36223–36229.

Chang AH, O'Shaughnessy MV, Jirik FR. 2001. Hck SH3 domain-dependent abrogation of Nef-induced class I MHC down-regulation. Eur J Immunol 31:2382–2387.

Chitu V, Stanley ER. 2006. Colony-stimulating factor-1 in immunity and inflammation. Curr Opin Immunol 18:39–48.

David-Pfeuty T, Nouvian-Dooghe Y. 1990. Immunolocalization of the cellular src protein in interphase and mitotic NIH c-src overexpresser cells. J Cell Biol 111:3097–3116.
Deacon NJ, Tsykin A, Solomon A, Smith K, Ludford-Menting M, Hooker DJ, McPhee DA, Greenway AL, Ellett A, Chatfield C, Lawson VA, Crowe S, Maerz A, Sonza S, Learmont, Sullivan JS, Cunningham A, Dwyer D, Mills J. 1995. Genomic structure of an attenuated quasi species of HIV-1 from a blood transfusion and recipients. Science 270:988–991.
Drakesmith H, Chen N, Ledermann H, Screaton G, Townsend A, Xu XN. 2005. HIV-1 Nef down-regulates the hemochromatosis protein HFE, manipulating cellular iron homeostasis. Proc Natl Acad Sci USA 102:11017–11022.
Fackler OT, Baur AS. 2002. Live and let die: Nef functions beyond HIV replication. Immunity 16:493–497.
Fackler OT, Wolf D, Weber HO, Laffert B, D'Aloja P, Schuler-Thurner B, Geffin R, Saksela K, Geyer M, Peterlin BM, Schuler G, Baur AS. 2001. A natural variability in the proline-rich motif of Nef modulates HIV-1 replication in primary T cells. Curr Biol 11:1294–1299.
Greenberg ME, lafrate AJ, Skowronski J. 1998. The SH3 domain-binding surface and an acidic motif in HIV-1 nef regulate trafficking of class I MHC complexes. EMBO J 17:2777–2789.
Haller C, Rauch S, Fackler OT. 2007. HIV-1 Nef employs two distinct mechanisms to modulate Lck subcellular localization and TCR induced actin remodeling. PLoS ONE 2:e1212.
Hamilton JA. 2008. Colony-stimulating factors in inflammation and autoimmunity. Nat Rev Immunol 8:533–544.
Hanna Z, Kay DG, Rebai N, Guimond A, Jothy S, Jolicoeur P. 1998. Nef harbors a major determinant of pathogenicity for and AIDS-like disease induced by HIV-1 in transgenic mice. Cell 95:163–175.
Hanna Z, Weng X, Kay DG, Poudrier J, Lowell C, Jolicoeur P. 2001. The pathogenicity of human immunodeficiency virus (HIV) type 1 Nef in CD4C/HIV transgenic mice is fabolished by mutation of its SH3-binding domain, and disease development is delayed in the absence of Hck. J Virol 75:9378–9392.
Hashimoto S, Hirose M, Hashimoto A, Morishige M, Yamada A, Hosaka H, Akagi K, Ogawa E, Oneyama C, Agatsuma T, Okada M, Kobayashi H, Wada H, Nakano H, Ikegami T, Nakagawa A, Sabe H. 2006. Targeting AMAP1 and cortactin binding bearing an atypical src homology 3/proline interface for prevention of breast cancer invasion and metastasis. Proc Natl Acad Sci USA 103:7036–7041.
Hiyoshi M, Suzu S, Yoshidomi Y, Hassan R, Harada H, Sakashita N, Akari H, Motoyoshi K, Okada S. 2008. Interaction between Hck and HIV-1 Nef negatively regulates cell surface expression of M-CSF receptor. Blood 111:243–250.
Hung CH, Thomas L, Ruby CE, Atkins KM, Morris NP, Knight ZA, Scholz I, Barklis E, Weinberg AD, Shokat KM, Thomas G. 2007. HIV-1 Nef assembles a Src family kinase-ZAP-70/Syk-PI3K cascade to down-regulate cell surface MHC-I. Cell Host Microbe 1:121–133.
Kaplan KB, Swedlow JR, Varmus HE, Morgan DO. 1992. Association of $p60^{c\text{-}src}$ with endosomal membranes in mammalian fibroblasts. J Cell Biol 118:321–333.
Karkkainen S, Hiipakka M, Wang JH, Kleino I, Vaha-Jaakkola M, Renkema GH, Kiss M, Wagner R, Saksela K. 2006. Identification of preferred protein interactions by phage-display of the human Src homology-3 proteome. EMBO Rep 7:186–191.
Kasahara K, Nakayama Y, Ikeda K, Fukushima Y, Matsuda D, Horimoto S, Yamaguchi N. 2004. Trafficking of Lyn through the Golgi caveolin involves the charged residues on αE and αI helices in the kinase domain. J Cell Biol 165:641–652.
Kestler HW III, Ringler DJ, Mori K, Panicali DL, Sehgal PK, Daniel MD, Desrosiers RC. 1991. Importance of the nef gene for maintenance of high virus loads and for development of AIDS. Cell 65:651–662.
Kirchhoff F, Greenough TC, Brettler DB, Sullivan JL, Desrosiers RC. 1995. Brief report: Absence of intact nef sequences in a long-term survivor with nonprogressive HIV-1 infection. N Engl J Med 332:228–232.
Korade-Mirnics Z, Corey SJ. 2000. Src kinase-mediated signaling in leukocytes. J Leukocyte Biol 68:603–613.
Lerner EC, Smithgall TE. 2002. SH3-dependent stimulation of Src-family kinase autophosphorylation without tail release from the SH2 domain in vivo. Nat Struct Biol 9:365–369.
Ley SC, Marsh M, Bebbington CR, Proudfoot K, Jordan P. 1994. Distinct intracellular localization of Lck and Fyn protein tyrosine kinases in human T lymphocytes. J Cell Biol 125:639–649.
Lowell CA. 2004. Src-family kinases: Rheostats of immune cell signaling. Mol Immunol 41:631–643.
Mangasarian A, Piguet V, Wang JK, Chen YL, Trono D. 1999. Nef-induced CD4 and major histocompatibility complex class I (MHC-I) down-regulation are governed by distinct determinants: N-terminal alpha helix and proline repeat of Nef selectively regulate MHC-I trafficking. J Virol 73:1964–1973.
Matsuda D, Nakayama Y, Horimoto S, Kuga T, Ikeda K, Kasahara K, Yamaguchi N. 2006. Involvement of Golgi-associated Lyn tyrosine kinase in the translocation of annexin II to the endoplasmic reticulum under oxidative stress. Exp Cell Res 312:1205–1217.
Mitina O, Warmuth M, Krause G, Hallek M, Obermeier A. 2007. Src family tyrosine kinases phosphorylate Flt3 on juxtamembrane tyrosines and interfere with receptor maturation in a kinase-dependent manner. Ann Hematol 86:777–785.
Moarefi I, LaFevre-Bernt M, Sicheri F, Huse M, Lee CH, Kuriyan J, Miller WT. 1997. Activation of the Src-family tyrosine kianse Hck by SH3 domain displacement. Nature 385:650–653.
Oneyama C, Agatsuma T, Kanda Y, Nakano H, Sharma SV, Nakano S, Narazaki F, Tatsuta K. 2003. Synthetic inhibitors of proline-rich ligand-mediated protein-protein interaction: Potent analogs of UCS15A. Chem Biol 10:443–451.
Paliwal P, Radha V, Swarup G. 2007. Regulation of p73 by Hck through kinase-dependent and independent mechanisms. BMC Mol Biol 8:45.
Peterlin BM, Trono D. 2003. Hide, shield and strike back: How HIV-infected cells avoid immune eradication. Nat Rev Immunol 3:97–107.
Priceputu E, Hanna Z, Hu C, Simard MC, Vincent P, Wildum S, Schindler M, Kirchhoff F, Jolicoeur P. 2007. Primary human immunodeficiency virus type 1 Nef alleles show major differences in pathogenicity in transgenic mice. J Virol 81:4677–4693.
Pulvirenti T, Giannotta M, Capestrano M, Capitani M, Pisanu A, Polishchuk RS, San Pietro E, Beznoussenko GV, Mironov AA, Turacchio G, Hsu VW, Sallese M, Luini A. 2008. A traffic-activated Golgi-based signaling circuit coordinates the secretory pathway. Nat Cell Biol 10:912–922.
Roeth JF, Collins KL. 2006. Human immunodeficiency virus type 1 Nef: Adapting to intracellular trafficking pathways. Mol Biol Rev 70:548–563.
Saksela K, Cheng G, Baltimore D. 1995. Proline-rich (PxxP) motifs in HIV-1 Nef bind to SH3 domains of a subset of Src kinases and are required for the enhanced growth of Nef^{+} viruses but not for down-regulation of CD4. EMBO J 14:484–491.
Schwartz O, Marechal V, Le Gall S, Lemonnier F, Heard JM. 1996. Endocytosis of major histocompatibility complex class I molecules is induced by the HIV-1 Nef protein. Nat Med 2:338–342.
Suzu S, Tanaka-Douzono M, Nomaguchi K, Yamada M, Hayasawa K, Kimura F, Motoyoshi K. 2000. $p56^{dok\text{-}2}$ as a cytokine-inducible inhibitor of cell proliferation and signal transduction. EMBO J 19:5114–5122.
Suzu S, Harada H, Matsumoto T, Okada S. 2005. HIV-1 Nef interferes with M-CSF receptor signaling through Hck activation and inhibits M-CSF bioactivities. Blood 105:3230–3237.
Trible RP, Emert-Sedlak L, Smithgall TE. 2006. HIV-1 Nef selecyively activates Src family kinases Hck, Lyn, and c-Src through SH3 domain interaction. J Biol Chem 281:27029–27038.
Ueno T, Motozono C, Dohki S, Mwimanzi P, Rauch S, Fackler OT, Oka S, Takiguchi M. 2008. CTL-mediated selective pressure influences dynamic evolution and pathogenetic functions of HIV-1 Nef. J Immunol 180:1107–1116.
van't Hof W, Resh MD, 1997. Rapid plasma membrane anchoring of newly synthesized p59fyn: Selective requirement for NH_2-terminal myristoylation and palmitoylation at cysteine-3. J Cell Biol 136:1023–1035.

Retrovirology

BioMed Central

Research

Open Access

Modification of a loop sequence between α-helices 6 and 7 of virus capsid (CA) protein in a human immunodeficiency virus type 1 (HIV-1) derivative that has simian immunodeficiency virus (SIVmac239) *vif* and CA α-helices 4 and 5 loop improves replication in cynomolgus monkey cells

Ayumu Kuroishi[1], Akatsuki Saito[2], Yasuhiro Shingai[1], Tatsuo Shioda[1], Masako Nomaguchi[3], Akio Adachi[3], Hirofumi Akari[2] and Emi E Nakayama*[1]

Address: [1]Department of Viral Infections, Research Institute for Microbial Diseases, Osaka University, Osaka 565-0871, Japan, [2]Tsukuba Primate Research Center, National Institute of Biomedical Innovation, Ibaraki 305-0843, Japan and [3]Department of Virology, Institute of Health Biosciences, University of Tokushima Graduate School, Tokushima 770-8503, Japan

Email: Ayumu Kuroishi - kuroishi@biken.osaka-u.ac.jp; Akatsuki Saito - a-saito@nibio.go.jp; Yasuhiro Shingai - chokobo918@tcct.zaq.ne.jp; Tatsuo Shioda - shioda@biken.osaka-u.ac.jp; Masako Nomaguchi - nomaguchi@basic.med.tokushima-u.ac.jp; Akio Adachi - adachi@basic.med.tokushima-u.ac.jp; Hirofumi Akari - akari@nibio.go.jp; Emi E Nakayama* - emien@biken.osaka-u.ac.jp

* Corresponding author

Published: 3 August 2009

Retrovirology 2009, **6**:70 doi:10.1186/1742-4690-6-70

Received: 12 March 2009
Accepted: 3 August 2009

This article is available from: http://www.retrovirology.com/content/6/1/70

Abstract

Background: Human immunodeficiency virus type 1 (HIV-1) productively infects only humans and chimpanzees but not cynomolgus or rhesus monkeys while simian immunodeficiency virus isolated from macaque (SIVmac) readily establishes infection in those monkeys. Several HIV-1 and SIVmac chimeric viruses have been constructed in order to develop an animal model for HIV-1 infection. Construction of an HIV-1 derivative which contains sequences of a SIVmac239 loop between α-helices 4 and 5 (L4/5) of capsid protein (CA) and the entire SIVmac239 *vif* gene was previously reported. Although this chimeric virus could grow in cynomolgus monkey cells, it did so much more slowly than did SIVmac. It was also reported that intrinsic TRIM5α restricts the post-entry step of HIV-1 replication in rhesus and cynomolgus monkey cells, and we previously demonstrated that a single amino acid in a loop between α-helices 6 and 7 (L6/7) of HIV type 2 (HIV-2) CA determines the susceptibility of HIV-2 to cynomolgus monkey TRIM5α.

Results: In the study presented here, we replaced L6/7 of HIV-1 CA in addition to L4/5 and *vif* with the corresponding segments of SIVmac. The resultant HIV-1 derivatives showed enhanced replication capability in established T cell lines as well as in CD8+ cell-depleted primary peripheral blood mononuclear cells from cynomolgus monkey. Compared with the wild type HIV-1 particles, the viral particles produced from a chimeric HIV-1 genome with those two SIVmac loops were less able to saturate the intrinsic restriction in rhesus monkey cells.

Conclusion: We have succeeded in making the replication of simian-tropic HIV-1 in cynomolgus monkey cells more efficient by introducing into HIV-1 the L6/7 CA loop from SIVmac. It would be of interest to determine whether HIV-1 derivatives with SIVmac CA L4/5 and L6/7 can establish infection of cynomolgus monkeys *in vivo*.

Background

Human immunodeficiency virus type 1 (HIV-1) productively infects only humans and chimpanzees but not Old World monkeys (OWM) such as cynomolgus (CM) and rhesus (Rh) monkeys [1]. Unlike the simian immunodeficiency virus isolated from macaques (SIVmac), HIV-1 replication is blocked early after viral entry, before the establishment of a provirus in OWM cells [1-3]. This restricted host range of HIV-1 has greatly hampered its use in animal experiments and has caused difficulties for developing prophylactic vaccines and understanding HIV-1 pathogenesis. In order to establish a monkey model of HIV-1/AIDS, various chimeric viral genomes between SIVmac and HIV-1 (SHIV) have been constructed and tested for their replicative capabilities in simian cells. The first SHIV was generated on a genetic background of SIVmac with HIV-1 *tat, rev, vpu,* and *env* genes [4]. Although such a SHIV is useful for the analysis of humoral immune responses against the Env protein [5-7], SHIVs containing other HIV-1 structural proteins, especially the Gag-Pol protein, have become highly desirable, since cellular immune response against Gag is generally believed to be important for disease control [8-10].

In recent years, several host factors involved in HIV-1 restriction in OWM cells have been identified. ApoB mRNA editing catalytic subunit (APOBEC) 3 G modifies the minus strand viral DNA during reverse transcription, resulting in an impairment of viral replication [11-13]. This activity could be counteracted with the viral protein Vif [14-17]. Although HIV-1 Vif can potently suppress human APOBEC3G, it is not effective against Rh APOBEC3G, which explains at least partly why HIV-1 replication is restricted in monkey cells. It is well known that Cyclophilin A (CypA) binds directly to the exposed loop between α-helices 4 and 5 (L4/5) of HIV-1 capsid protein (CA), but not to the SIVmac CA. Several studies have found that CypA augments HIV-1 infection in human cells but inhibits its replication in OWM cells [18-20]. A construction of a SHIV with a minimal segment of SIVmac was reported recently by Kamada et al. [21]. This SHIV was designed to evade the restrictions mediated by APOBEC3G and CypA in OWM cells and contains the 7-aa segment corresponding to the L4/5 of CA and the entire *vif* of SIVmac. The SHIV was found to be able to replicate in primary CD4+ T cells from pig-tailed monkey as well as in the CM HSC-F T cell line. Both in HSC-F and in primary CD4+ T cells, this chimeric virus grew to lower titers than did SIVmac [21]; and when inoculated into pig-tailed monkeys, this SHIV did not cause CD4+ T cell depletion or any clinical symptoms in the inoculated animals [22]. Another SHIV, stHIV-1 (a virus carrying 202 amino acid residues of SIVmac CA and *vif* generated by Hatziioannou et al.) could replicate efficiently in Rh cells [23]. However, long-term passaging in Rh cells was necessary to generate an efficiently replicating stHIV-1, and this adapted virus has not yet been fully characterized; so it may be that further modifications of the viral genome are necessary for optimal replication of HIV-1 genomes in OWM cells.

TRIM5α, a member of the tripartite motif (TRIM) family proteins, was identified in 2004 as another intrinsic restriction factor of HIV-1 in OWM cells [24]. Rh and CM TRIM5α were found to restrict HIV-1 but not SIVmac [25,26]. TRIM5α recognizes the multimerized CA of an incoming virus by its α-isoform specific SPRY domain [27-29] and is believed to be involved in innate immunity to control retroviral infection [30]. Previously, Ylinen et al. mapped one of the determinants of TRIM5α sensitivity in L4/5 of HIV type 2 (HIV-2) CA [31]. In addition, we identified a single amino acid of the surface-exposed loop between α-helices 6 and 7 (L6/7) of HIV-2 CA as a determinant of the susceptibility of HIV-2 to CM TRIM5α [32]. We hypothesized that the L6/7 of HIV-1 CA also determines susceptibility to CM TRIM5α. Here, we investigated whether an additional replacement of L6/7 of HIV-1 CA with that of SIVmac would enhance the replication capability of a SHIV genome in established T cell line HSC-F and in CD8+ cell depleted peripheral blood mononuclear cells (PBMCs) from CMs.

Materials and methods

DNA constructions

The HIV-1 derivatives were constructed on a background of infectious molecular clone NL4-3 [33]. NL-ScaVR, a virus containing SIVmac239 L4/5 and the entire vif gene, was constructed according to the procedure described by Kamada et al. [21]. A single amino acid His (H) at the 120th position of NL-ScaVR CA was replaced with Gln (Q) by means of site-directed mutagenesis with the PCR-mediated overlap primer extension method [34], and the resultant construct was designated NL-ScaVRA1. The L6/7 of CA (HNPPIP) of NL-SVR, NL-ScaVR, or NL-DT5R was also replaced with the corresponding segments of SIVmac239 CA (RQQNPIP) by means of site-directed mutagenesis, and the resultant constructs were designated NL-SVR6/7S, NL-ScaVR6/7S, or NL-DT5R6/7S, respectively. The BssHII-ApaI fragment of NL-ScaVR, NL-SVR6/7S, or NL-ScaVR6/7S, which corresponds to matrix (MA) and CA, was transferred to env deleted NL4-3 (NL-Nhe) to generate the env (-) version of each of the constructs.

Cells and Virus propagation

The 293 T (human kidney), LLC-MK2 (Rh kidney), and TK-ts13 (hamster kidney) adherent cell lines were cultured in Dulbecco's modified Eagle medium supplemented with 10% heat-inactivated FBS. The CD4+ CXCR4+ CM T cell line HSC-F [35] was maintained in RPMI 1640 medium containing 10% FBS. Virus stocks were prepared by transfection of 293 T cells with HIV-1

NL4-3 derivatives using the calcium phosphate co-precipitation method. Viral titers were measured with the p24 or p27 RetroTek antigen ELISA kit (ZeptoMetrix, Buffalo, NY), and viral reverse transcriptase (RT) was quantified with the Reverse Transcriptase Assay kit (Roche Applied Science, Mannheim Germany).

Green fluorescence protein (GFP) vector

The HIV-1 vector expressing GFP was prepared as described previously [36,37]. To construct the HIV-1-WT-GFP and HIV-1-L4/5S-GFP vector, we replaced the Eco RI-Apa I fragment corresponding to MA and CA of the pMDLg/p.RRE packaging vector with those fragments from NL4-3 and NL-ScaVR, respectively. The GFP viruses were prepared from 293 T cells in a 15-cm dish by co-transfection with a combination of 24 μg of pMDLg/p.RRE derivatives, 36 μg of CS-CDF-CG-PRE (GFP encoding viral genomic plasmid), 10 μg of pMD.G (vesicular stomatitis virus glycoprotein (VSV-G) expressing plasmid), and 10 μg of pRSV-Rev (Rev expressing plasmid). Forty-eight hours after transfection, the culture supernatants were collected and used for infection.

Viral infections

3×10^5 MT4 or HSC-F cells were infected with 20 ng of p24 of NL4-3, NL-ScaV, NL-ScaVR, NL-ScaVR6/7S, NL-DT5R, or NL-DT5R6/7S. The culture supernatants were collected periodically, and p24 levels were measured with an ELISA kit.

Particle purification and Western blotting

The culture supernatant of 293 T cells transfected with plasmids encoding HIV-1 NL4-3 derivatives was clarified by means of low speed centrifugation. Nine ml of the resultant supernatants were layered onto a 2 ml cushion of 20% sucrose (made in PBS) and centrifuged at 35,000 rpm for 2 h in a Beckman SW41 rotor. After centrifugation, the virion pellets were resuspended in PBS, and p24 antigen concentrations were measured with ELISA. SDS-polyacrylamide gel electrophoresis was applied to 120 ng of p24 of HIV-1 derivatives, and virion-associated proteins were transferred to a PVDF membrane. CA and CypA proteins were visualized with the anti-p24 antibody (Biodesign International, Saco, ME) and the anti-CypA antibody (Affinity BioReagents, Golden, CO), respectively.

Saturation assay

HIV-1 derivatives or SIVmac particles were prepared by transfecting each of the env-deleted HIV-1 NL4-3 derivatives or SIVmac plasmids with a plasmid encoding VSV-G into 293 T cells, and culture supernatants were collected two days after transfection. One day before infection, Rh LLC-MK2 and hamster TK-ts13 were plated at a density of 5×10^4 cells per well in a 24-well plate. Prior to GFP virus infection, the cells were pretreated for 2 hours with 200 ng of p24 of each of the HIV-1 or SIVmac particles pseudotyped with VSV-G. Immediately after the pre-treatment, the cells were washed and infected with the HIV-1-WT-GFP or HIV-1-L4/5S-GFP virus. Two hours after infection, the inoculated GFP viruses were washed, and the cells were cultivated in fresh media. Two days after infection, the cells were fixed by formaldehyde, and GFP expressing cells were counted with a flowcytometer. To suppress endogenous TRIM5α activity, the cells were first infected with Sendai (SeV) expressing TRIM5 lacking the SPRY domain at a multiplicity of infection of 10 plaque forming units per cell. Sixteen hours after SeV infection, the cells were treated with 200 ng of p24 of the particles and then infected with the HIV-1-L4/5S-GFP vector as described above.

Preparation of CD8-depleted CM PBMCs and viral infection

CM PBMCs were suspended in RPMI medium 1640 supplemented with 10% (vol/vol) FBS, and the CD8+ cells were removed with a magnetic bead system (Miltenyi Biotec, Auburn, CA) and stimulated for 1 day with 1 μg/ml of PHA-L (Sigma, St. Louis. MO). For prolonged stimulation, CD8-depleted CM PBMCs were first stimulated with 1 μg/ml of PHA-L for 2 days and then with human IL2 100 U/ml for 2 more days. 3×10^5 cells were then inoculated with 200 ng of p24 of NL-DT5R, NL-DT5R6/7S or with 200 ng of p27 of SIVmac239 and incubated at 37°C in a medium containing 100 U/ml of human IL2. The culture supernatants were collected periodically, and the levels of p24 or p27 were measured with an antigen capture assay (Advanced BioScience Laboratories, Kensington, MD)

Results

Construction and characterization of HIV-1 molecular clones containing CA and Vif sequences from SIVmac239

Several proviral DNA constructs have been generated to counteract the restriction of HIV-1 replication in CM T cell line HSC-F [38] (Fig. 1). We first generated NL-SVR and NL-ScaVR according to the procedure described by Kamada et al. [21]. NL-ScaVR, a virus with SIVmac239 L4/5 CA and *vif*, could replicate slowly in HSC-F and replicated well in MT4 as previously reported (Fig. 2A). We recently discovered that the 120th amino acid of CA affected the sensitivity of HIV-2 to CM TRIM5α [32]. We, therefore, introduced an additional amino acid substitution, His to Gln, at this position in NL-ScaVR. The resultant virus was designated NL-ScaVRA1; but this virus unexpectedly showed less efficient replication than did the parental NL-ScaVR in both MT4 and HSC-F cells (Fig. 2A), probably due to a reduced viral fitness created by this mutation. We, therefore, replaced the entire L6/7 CA of NL-ScaVR (HNPPIP) with the corresponding loop from SIVmac239 (RQQNPIP), and the resultant virus was des-

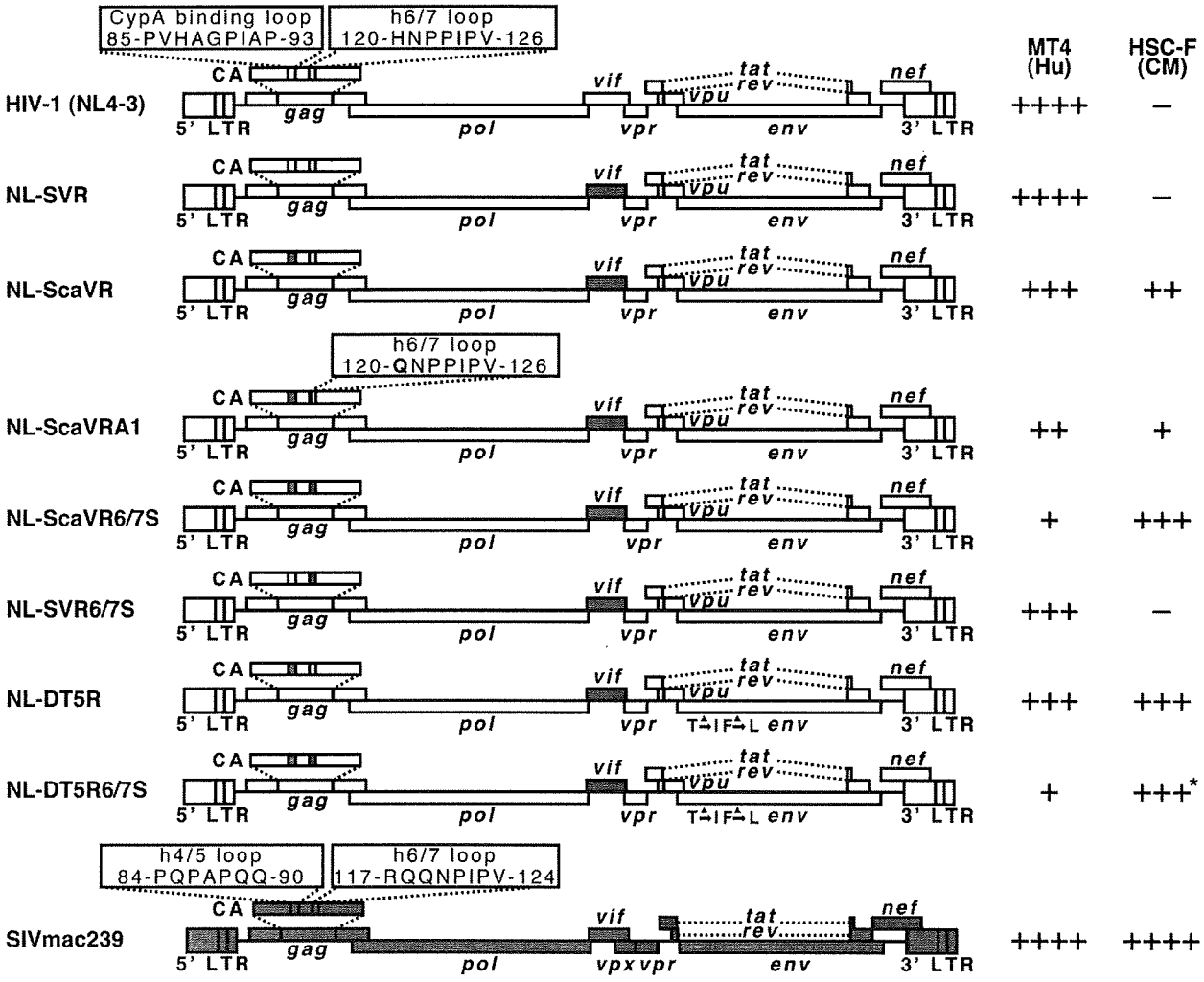

Figure 1

Structure of the chimeric HIV-1/SIVmac clones and a summary of their replication capabilities. White bars denote HIV-1 (NL4-3) and gray bars SIVmac239 sequences. ++++, +++, ++, +, and -denote the peak titer of virus growth in human (Hu) and cynomolgus monkey (CM) cells, respectively, to more than 1000 ng/ml, 100–1000 ng/ml, 10–100 ng/ml, 1–10 ng/ml, and less than 1 ng/ml concentration of capsid (CA) protein in the culture supernatants. * denotes that NL-DT5R6/7S replicated faster in HSC-F than did the parental NL-DT5R (see Fig. 2C).

ignated NL-ScaVR6/7S. The amount of RT per 1 ng of CA of NL-ScaVR (0.083 ng) was comparable to that of NL-ScaVR6/7S (0.081 ng), indicating that the replacement of L6/7 in HIV-1 with the corresponding loop of SIVmac did not affect the reactivity of CA antigen. Although NL-ScaVR6/7S grew slightly slower in MT4 cells, it could replicate more efficiently in HSC-F cells than the parental NL-ScaVR could (Fig. 2A). Similar results were obtained when we inoculated 20 ng of RT equivalent of NL-ScaVR or NL-ScaVR6/7S into HSC-F cells and measured the periodic RT production in culture supernatants (data not shown). These findings demonstrated that L6/7 CA of SIVmac improved the replication in CM cells of an HIV-1 derivative that already contained a SIVmac L4/5 and *vif*. We then generated NL-SVR6/7S, in which the L4/5 sequence was from HIV-1, but the L6/7 and *vif* came from SIVmac. NL-SVR6/7S showed better replication than NL-ScaVR6/7S in MT4 cells, but lost its replicative capability in HSC-F cells (Fig. 2B). NL-SVR, a virus with SIVmac *vif*, could replicate in MT4, but failed to do so in HSC-F (Fig. 2B). These results indicated that both L4/5 and L6/7 of SIVmac are required for efficient replication in HSC-F.

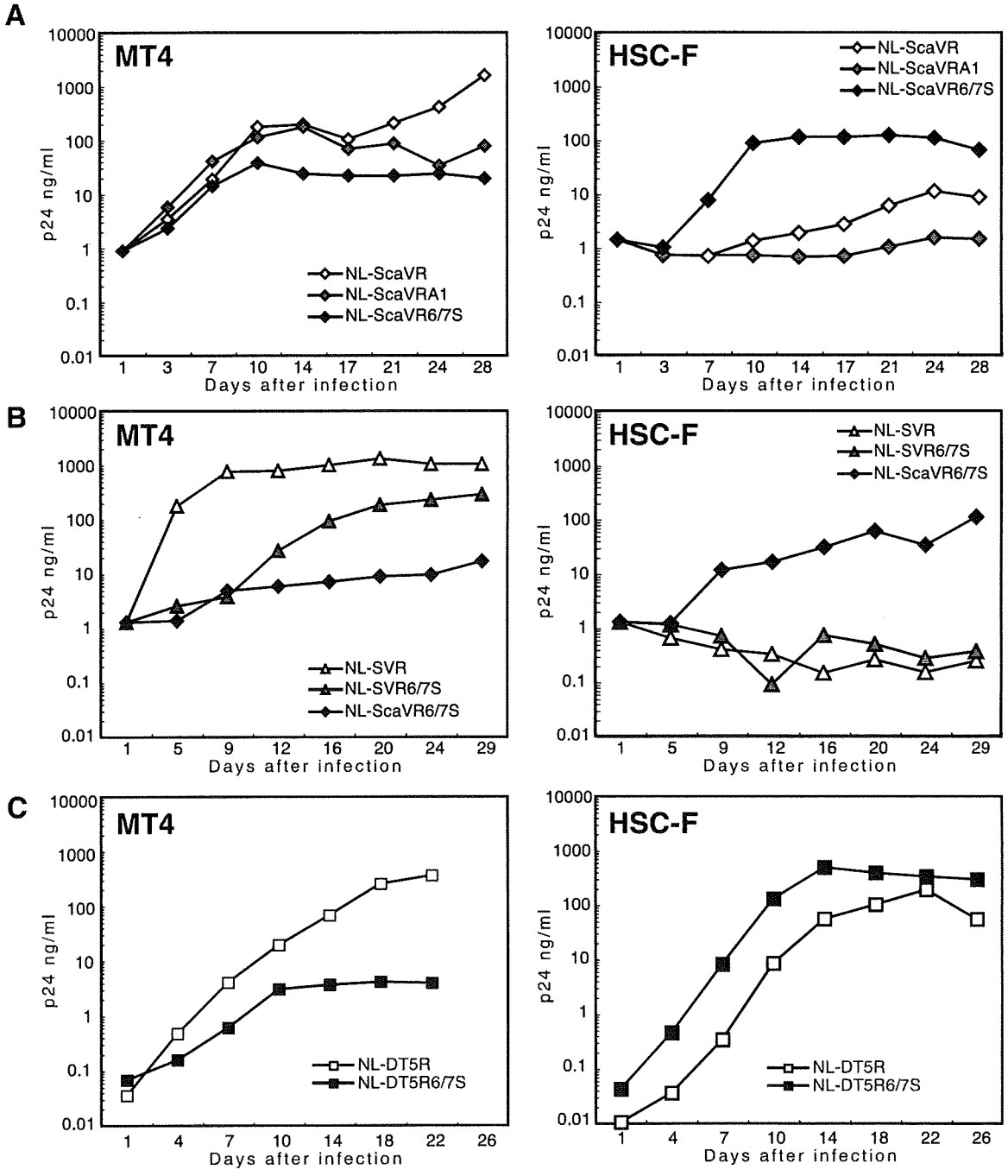

Figure 2
Replication properties of HIV-1 derivatives. Equal amounts of (A) NL-ScaVR (white diamonds: virus with SIVmac L4/5 and *vif*), and NL-ScaVRA1 (gray diamonds: virus with additional replacement of the 120th amino acid His with Gln in NL-ScaVR), and NL-ScaVR6/7S (black diamonds: virus with SIVmac L4/5, L6/7, and *vif*) (B) NL-SVR, NL-ScaVR6/7S, and NL-SVRS6/7S (gray diamonds: virus with SIVmac L6/7 and *vif*), and (C) NL-DT5R (white squares) and NL-DT5R6/7S (black squares), were inoculated into human MT4 or CM HSC-F cells, and culture supernatants were collected periodically. p24 antigen levels were measured by ELISA.

We then introduced SIVmac L6/7 into NL-DT5R, a molecularly cloned virus with two nonsynonymous changes in the *env* gene gained during long-term passages of NL-ScaVR in HSC-F cells [21]. The resultant virus was designated NL-DT5R6/7S. Although the peak titer of NL-DT5R6/7S was almost the same as that of NL-DT5R, NL-DT5R6/7S could replicate faster in HSC-F than the parental NL-DT5R (Fig. 2C). This finding confirmed that SIVmac L6/7 CA sequence improved the replication in CM cells of HIV-1 derivatives that contained SIVmac L4/5 and *vif*. The finding suggested that HIV-1 L6/7 and L4/5 CA sequences are important for intrinsic restriction in CM cells.

CypA incorporation into virus particles was not affected by replacement of HIV-1 L6/7 with that of SIVmac

Several studies have demonstrated that CypA augments HIV-1 infection in human cells [39], but inhibits its replication in OWM cells [18-20]. CypA was packaged in HIV-1 but not in SIVmac virus particles. To determine whether the replacement of HIV-1 L6/7 with that of SIVmac affects CypA binding of HIV-1 CA, we performed Western blot analysis of viral particles from HIV-1 derivatives. As shown in Fig. 3 (upper panel), CypA proteins were clearly detected in the NL-SVR particles (lane 1) but not in those of NL-ScaVR (lane 3), thus confirming that the L4/5 sequence of HIV-1 but not of SIVmac is required for CypA incorporation into viral particles. CypA proteins were detected in NL-SVR6/7S (lane 2) but not in NL-ScaVR6/7S (lane 4), indicating that the additional replacement of HIV-1 L6/7 with that of SIVmac had little effect on CypA incorporation. This finding suggests that the effect of L6/7 replacement on viral growth was independent from CypA binding of HIV-1 CA. When we used anti-p24 antibody (Fig. 3, lower panel), p55 Gag precursors and p24 proteins were clearly detected. There were no differences in the amount of p24 or the ratio of p24 to p55 among the four HIV-1 derivatives, indicating that the HIV-1 Gag precursor proteins with SIVmac L4/5 and L6/7 were processed normally by the viral protease.

Replacement of both L4/5 and L6/7 of HIV-1 CA with the corresponding loops from SIVmac impaired the CA binding activity of TRIM5α in Rh cells

It is known that the intrinsic restriction factors working against HIV-1 in CM and Rh cells can be saturated by inoculation of a high dose of HIV-1 particles [19,40-42]. To determine whether alteration in the CA of HIV-1 would affect its ability to saturate restriction factors, Rh LLC-MK2 cells were pre-treated with equal amounts of VSV-G pseudotyped HIV-1 particles that were with or without SIVmac L4/5 and/or L6/7 CA to saturate intrinsic restriction factor(s). The pre-treated cells were then infected with GFP-expressing HIV-1 carrying SIVmac L4/5 CA (HIV-1-L4/5S-GFP), since we wanted to exclude any effects of CypA on

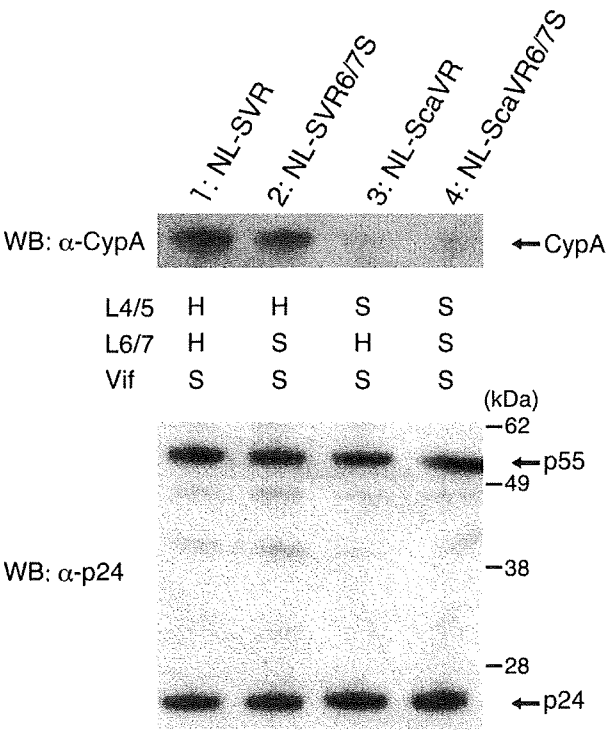

Figure 3
Western blot analysis of CA and CypA in particles of HIV-1 derivatives. The viral particles of NL-SVR (lane 1), NL-SVR6/7S (lane 2), NL-ScaVR (lane 3) and NL-ScaVR6/7S (lane 4) were purified by ultracentrifugation through a 20% sucrose cushion. CypA (upper panel) and p24 and p55 proteins (lower panel) were visualized by Western blotting (WB) using anti-CypA and anti-p24 antibody, respectively. "H" and "S" denote the amino acid sequences derived from HIV-1 and SIVmac, respectively.

the GFP expressing virus in LLC-MK2 cells. The susceptibility of particle-treated cells to virus infection was determined by the percentage of GFP-positive cells. The cells treated with the wild type (WT) particles showed greatly enhanced susceptibility to HIV-1 infection compared with non-treated cells (Fig. 4A, left), demonstrating that the intrinsic restriction factor(s) in LLC-MK2 cells were saturated by a high dose of particles. The cells treated with the particles carrying SIVmac L4/5 and those treated with particles carrying SIVmac L6/7 also showed enhanced susceptibility to HIV-1 infection (Fig. 4A, left). The cells treated with particles carrying both SIVmac L4/5 and L6/7 showed only slight enhancement of HIV-1 susceptibility (Fig. 4A, left; $p = 0.007$ compared by means of paired t test using all data points with the WT particle treated cells). Similarly, the cells treated with SIVmac particles showed only minor enhancement in HIV-1 susceptibility (Fig. 4A, left). Hamster TK-ts13 cells which lack TRIM5α expres-

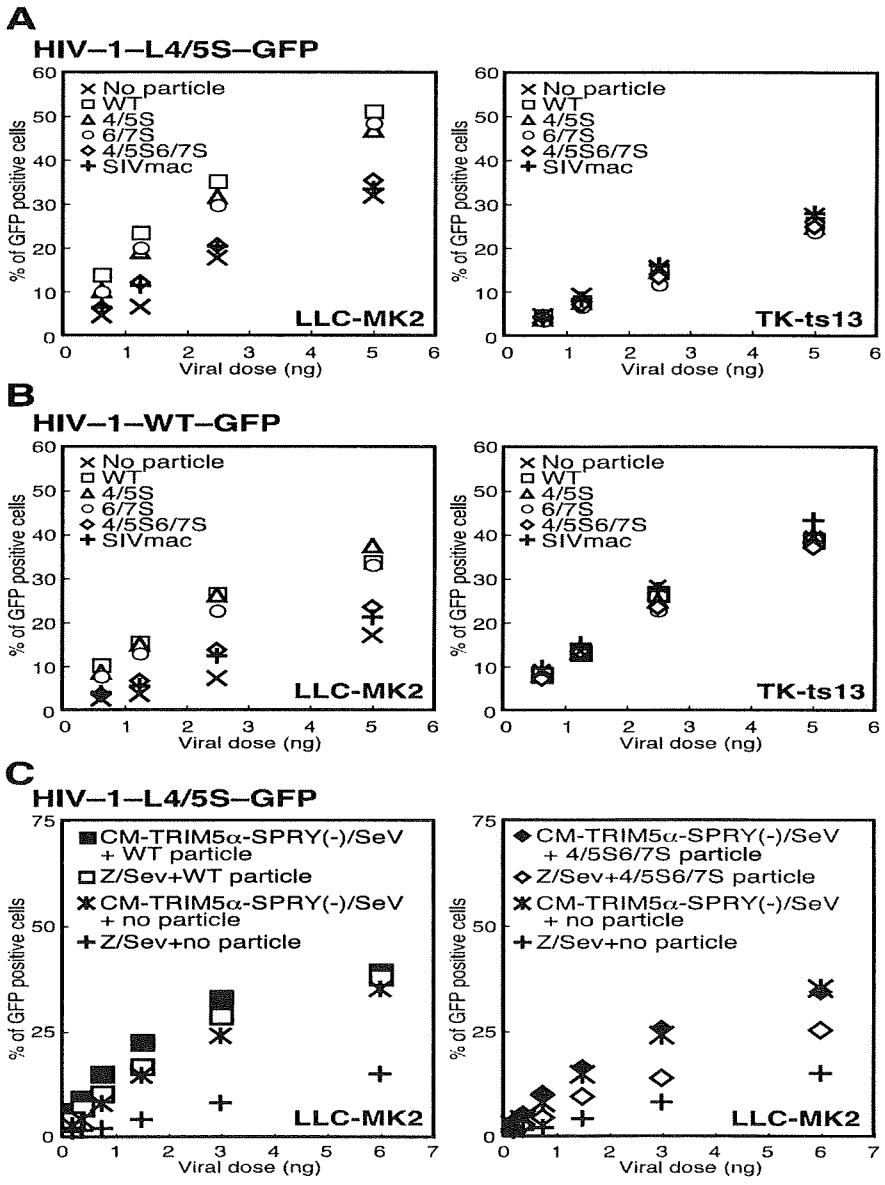

Figure 4

Saturation of intrinsic antiviral factors resulting from inoculation of high dose of virus particles. (A) Rhesus LLC-MK2 cells or hamster TK-ts13 cells were pre-treated with equal amounts of VSV-G pseudotyped particles with WT HIV-1 (white squares: Wt), with SIVmac L4/5 (white triangles: 4/5S), with SIVmac L6/7 (white circles: 6/7S), with SIVmac L4/5 and L6/7 (white diamonds: 4/5S6/7S), with SIVmac239 (pluses: SIVmac) or none (crosses) for 2 hours. The cells were then infected with the GFP expressing HIV-1 vector carrying SIVmac L4/5 (A: HIV-1-L4/5S-GFP) or GFP expressing HIV-1 vector with WT capsid (B: HIV-1-WT-GFP). Representative data of four independent experiments are shown. (C) Saturation activities were assessed in the presence or absence of functional TRIM5α. Before particle treatment, cells were infected with Sendai virus (SeV) expressing TRIM5 without the SPRY domain (black symbols), or an empty vector, parental Z strain of SeV (white symbols). Sixteen hours after SeV infection, cells were treated with particles for 2 hours and then infected with HIV-1-L4/5S-GFP. Representative data from six independent experiments are shown.

sion, on the other hand, showed no difference in HIV-1 susceptibility among cells treated with various HIV-1 derivatives or SIVmac particles (Fig. 4A, right). As shown in Fig. 4B, similar results were obtained when we used a GFP-expressing virus with WT HIV-1 capsid (HIV-1-WT-GFP). These results indicate that both HIV-1 L4/5 and L6/7 are important for CA binding to antiviral factor(s) in Rh cells. As described previously [20], HIV-1-WT-GFP could induce infection in only small numbers of LLC-MK2 cells. In contrast, more TK-ts13 cells were infected with HIV-1-WT-GFP than with HIV-1-L4/5-GFP. It is thus possible that CypA is a supporting factor for HIV-1 replication in hamster cells as well as in human cells.

Endogenous TRIM5α seems to be a likely candidate for the antiviral factor saturated by a high dose of HIV-1 particles (Fig. 4A and 4B). To confirm this, we assessed the ability of WT and mutant HIV-1 particles to saturate the intrinsic restriction factor in the presence or absence of functional TRIM5α. The dominant negative effect of an over-expressed TRIM5 mutant lacking SPRY domain [43] was used to suppress the function of cell endogenous TRIM5α. As shown in Fig. 4C, the infection of a recombinant SeV expressing TRIM5 without the SPRY domain caused marked enhancement of HIV-1-L4/5S-GFP virus infection without prior particle treatment (crosses vs. asterisks). This indicates that this dominant negative

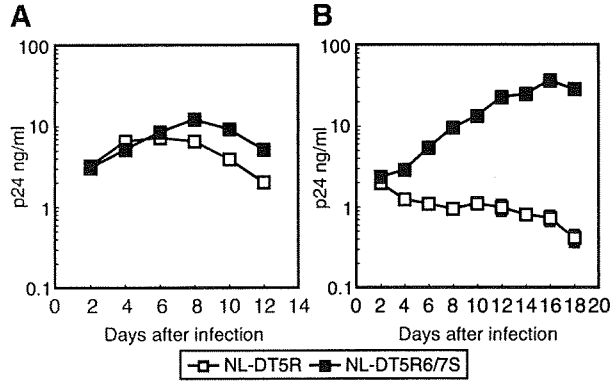

Figure 5
Replication capabilities of HIV-1 derivatives in peripheral blood mononuclear cells (PBMC) from CM. (A) PBMCs were obtained from CM, after which the CD8+ cells were removed, and the cells were stimulated with PHA-L for 1 day. (B) CD8-depleted CM PBMC were first stimulated with 1 μg/ml of PHA-L for 2 days and then with human IL2 100 U/ml for 2 more days. Equal amounts of p24 of NL-DT5R (white squares) or NL-DT5R6/7S (black squares) were inoculated, and the culture supernatants were collected periodically. p24 antigen levels were measured by ELISA. Values represent means with actual fluctuations of duplicate samples added. The values for mock infected cell culture supernatants were zero in the ELISA assay.

TRIM5 mutant successfully suppressed the restriction activity of endogenous TRIM5α. Treatment with the WT HIV-1 particles also saturated the restriction factors in the cells infected with the empty vector virus (parental Z strain of SeV), while the additional effect of the dominant negative mutant TRIM5α remained unclear (Fig. 4C left, white vs. black squares). These results suggest that the intrinsic factors saturated by the WT particles were mainly endogenous TRIM5α. In contrast to the effect of the WT particle treatment, the effect of the dominant negative TRIM5 mutant on HIV-1 infection was evident when we used particles with SIVmac L4/5 and L6/7 (Fig. 4C, right, white vs. black diamonds, $p = 0.007$, paired t test). These findings suggest that the diminished capability of particles with SIVmac L4/5 and L6/7 to saturate restriction factors was mainly due to their loss of interaction with TRIM5α. We, therefore, concluded that the ability of HIV-1 with SIVmac L4/5 and L6/7 to bind to TRIM5α is diminished in LLC-MK2 cells.

HIV-1 derivative with SIVmac L4/5, L6/7, and vif sequences can replicate efficiently in monkey primary cells

To verify the effect of additional replacement of HIV-1 L6/7 with that of SIVmac in primary CM cells, we prepared PBMCs from CM and removed CD8+ cells by means of magnetic beads. The cells were then stimulated for 1 day with 1 μg/ml of PHA-L. NL-DT5R6/7S showed more efficient replication than did the parental NL-DT5R in these cells and reached its peak titer 8 days after infection (Fig. 5A). For prolonged stimulation, CD8-depleted CM PBMCs were first stimulated with 1 μg/ml of PHA-L for 2 days and then with human IL2 100 U/ml for 2 more days. In these cells, NL-DT5R with HIV-1 L6/7 did not grow at all. On the other hand, NL-DT5R with SIVmac L6/7 (NL-DT5R6/7S) grew in CM primary cells in response to prolonged stimulation by PHA and IL-2 to reach titers, similar to those attained in cells with short stimulation, up to 8 days after infection (Fig. 5A and 5B). Furthermore, NL-DT5R6/7S continued to grow to much higher titers and reached its peak titer 16 days after infection; this higher peak may be due to better proliferation of these cells than those cells receiving short term stimulation (Fig. 5B). These results confirmed that the replicative capability of HIV-1 in CM cells was augmented by the additional replacement of L6/7 of CA with the corresponding sequence from SIVmac.

Discussion

We created simian-tropic HIV-1 with more efficient replication capability in CM cells using the knowledge obtained from our previous study of TRIM5α and HIV-2 capsid sequence variations [32] Introduction of the entire SIVmac L6/7 CA into the previously constructed version of HIV-1 derivatives containing SIVmac L4/5 CA and *vif* [21] caused only a four amino acid change in CA but